Lovász Principle for Unsupervised Graph Representation Learning

Ziheng Sun[1,2] **Chris Ding**[1] **Jicong Fan** [1,2*]
[1]School of Data Science, The Chinese University of Hong Kong, Shenzhen, China
[2]Shenzhen Research Institute of Big Data, Shenzhen, China
zihengsun@link.cuhk.edu.cn {chrisding,fanjicong}@cuhk.edu.cn

Abstract

This paper focuses on graph-level representation learning that aims to represent graphs as vectors that can be directly utilized in downstream tasks such as graph classification. We propose a novel graph-level representation learning principle called Lovász principle, which is motivated by the Lovász number in graph theory. The Lovász number of a graph is a real number that is an upper bound for graph Shannon capacity and is strongly connected with various global characteristics of the graph. Specifically, we show that the handle vector for computing the Lovász number is potentially a suitable choice for graph representation, as it captures a graph's global properties, though a direct application of the handle vector is difficult and problematic. We propose to use neural networks to address the problems and hence provide the Lovász principle. Moreover, we propose an enhanced Lovász principle that is able to exploit the subgraph Lovász numbers directly and efficiently. The experiments demonstrate that our Lovász principles achieve competitive performance compared to the baselines in unsupervised and semi-supervised graph-level representation learning tasks. The code of our Lovász principles is publicly available on GitHub[†].

1 Introduction

Graphs, such as chemical compounds, protein structures, and social networks, are non-Euclidean data that represent the relationships between entities. There have been a large number of previous works studying many aspects of graphs, including mutagenicity prediction of chemical compounds [Debnath *et al.*, 1991; Kriege and Mutzel, 2012], protein structure prediction [Borgwardt *et al.*, 2005], and community analysis of social networks [Yanardag and Vishwanathan, 2015].

Graph-based learning problems can be organized into two categories: node-level learning and graph-level learning. In this paper, we will only focus on graph-level learning. It is known that in graph-level learning, one fundamental task or step is to measure the distance or similarity between graphs. An important class of methods comparing graphs is graph kernel and many graph kernels have been proposed in the past decades [Siglidis *et al.*, 2020]. For instance, random walk kernels [Gärtner *et al.*, 2003] are the most widely-used and well-studied graph kernel family, which measure the graph similarity by counting the common random walks between graphs. The Weisfeiler-Lehman [Weisfeiler and Leman, 1968] family kernels are based on node label reassignment. Most graph kernels extract the similarity information between graphs by sampling sub-structures of graphs such as walks or reassigning the attributes of nodes with their neighborhoods. Note that graph kernels are implicit graph representation methods and hence their flexibilities are not high. In addition, the time and space complexities are quadratic with the number of graphs.

[*] Corresponding author

[†] https://github.com/SunZiheng0/Lovasz-Principle

37th Conference on Neural Information Processing Systems (NeurIPS 2023).

https://doi.org/10.52202/075280-2540

Graph representation learning aims to convert data with graph structure into vector representations that can be applied to various downstream tasks, such as graph clustering and classification. Many studies have been conducted on graph-level representation learning, and some of them use neural message-passing algorithms [Kipf *et al.*, 2018; Xie and Grossman, 2018; Gilmer *et al.*, 2017]. For instance, the InfoGraph proposed by [Sun *et al.*, 2019] achieves graph-level representations by maximizing the mutual information between the graph-level representation and the node-level representations. Graph contrastive learning (GraphCL) [You *et al.*, 2020] and adversarial graph contrastive learning (AD-GCL) [Suresh *et al.*, 2021] obtain graph-level representations by training graph neural networks (GNNs) to maximize the correspondence between the same graph's representations in its various augmented forms. JOint Augmentation Optimization (JOAO) [You *et al.*, 2021] is a framework that automatically and adaptively selects data augmentations for GraphCL on specific graph data, using a unified bi-level min-max optimization approach. Automated Graph Contrastive Learning (AutoGCL) [Yin *et al.*, 2022] uses learnable graph view generators and auto-augmentation strategy to generate contrastive samples while preserving the most representative structures of the original graph. These graph-level representation learning methods are all based on the InfoMax principle [Linsker, 1988]. Note that there are many other graph representation learning methods such as VGAE [Kipf and Welling, 2016; Hamilton *et al.*, 2017; Cui *et al.*, 2020], graph embedding [Wu *et al.*, 2020; Yu *et al.*, 2021; Bai *et al.*, 2019; Verma and Zhang, 2019], self-supervised learning [Liu *et al.*, 2022; Hou *et al.*, 2022; Lee *et al.*, 2022; Xie *et al.*, 2022; Wu *et al.*, 2021; Rong *et al.*, 2020; Zhang *et al.*, 2021b,a; Xiao *et al.*, 2022], and contrastive learning [Le-Khac *et al.*, 2020; Qiu *et al.*, 2020; Ding *et al.*, 2022; Xia *et al.*, 2022; Fang *et al.*, 2022; Trivedi *et al.*, 2022; Han *et al.*, 2022; Mo *et al.*, 2022; Yin *et al.*, 2022; Xu *et al.*, 2021; Zhao *et al.*, 2021; Zeng and Xie, 2021; Li *et al.*, 2022a,b; Wei *et al.*, 2022], which will not be detailed in this paper due to the page length limit.

The InfoMax principle [Linsker, 1988], which is very popular in graph-level representation learning, advocates maximizing the mutual information between the representations of entire graphs and the representations of substructures of varying sizes [Peng *et al.*, 2020; Velickovic *et al.*, 2019; Hassani and Khasahmadi, 2020; Xie *et al.*, 2022; Qiu *et al.*, 2020]. These InfoMax-based methods usually evaluate the mutual information (MI) between different representations using Jensen-Shannon MI estimator [Sun *et al.*, 2019], following the formulations of f-GAN [Nowozin *et al.*, 2016] and Mutual Information Neural Estimation (MINE) [Belghazi *et al.*, 2018]. However, the Jensen-Shannon MI estimator necessitates the training of a neural network parameterized discriminator, which is overly complex. In addition, the estimator is based on sampling, which may not be accurate enough in exploiting the mutual information. As opposed to InfoMax, researchers proposed the graph information bottleneck (GIB) [Wu *et al.*, 2020] and the subgraph information bottleneck (SIB) [Yu *et al.*, 2021] that aim to learn the minimal sufficient representation for downstream tasks. But GIB [Wu *et al.*, 2020] and SIB [Yu *et al.*, 2021] may fail if the downstream tasks are not available in the representation learning stage.

In this work, we introduce a novel graph learning principle called Lovász principle, which is inspired by the Lovász number [Lovász, 1979] in graph theory. The Lovász number is an upper bound for a graph's Shannon capacity. It is closely associated with various global characteristics of a graph, such as the clique number and chromatic number of the complement graph. The handle vector for calculating the Lovász number is potentially a suitable choice for the graph-level representation, as it captures a graph's global features, though it suffers from a few difficulties. The contributions of this work are summarized as follows.

- We propose the Lovász principle, a novel framework for unsupervised graph representation learning. We show how to effectively and efficiently utilize the handle vectors to represent graphs. The Lovász principle exploits the topological structures of graphs globally via neural networks.
- We propose an enhanced Lovász principle via effectively incorporating subgraph Lovász numbers, while direct computation of subgraph Lovász numbers is extremely costly. The enhanced Lovász principle ensures similar graphs have similar representations.
- We extend the Lovász principles to semi-supervised representation learning. Note that it is possible to adapt the Lovász principles to more graph-based learning problems.

The experimental results of unsupervised learning, semi-supervised learning, and transfer learning on many benchmark graph datasets show that the proposed Lovász principles outperform graph kernels, classical graph embedding methods, and InfoMax principle based representation learning methods.

https://doi.org/10.52202/075280-2540

2 Notations and Preliminaries

In this work, we use x, $\boldsymbol{x}$, $\boldsymbol{X}$, $\mathcal{X}$ (or X) to denote scalar, vector, matrix, and set respectively. $\mathbf{1}_{a\times b}$ is a matrix of size $a \times b$ consisting only ones. $\boldsymbol{I}_n$ denotes an identity matrix of size $n \times n$. Let $G = (V, E)$ be a graph with n nodes and a-dimensional node features $\{\boldsymbol{x}_v \in \mathbb{R}^a | v \in V\}$. We denote $\boldsymbol{A} \in \mathbb{R}^{n\times n}$ as the adjacency matrix and $\boldsymbol{X} = [\boldsymbol{x}_1, ..., \boldsymbol{x}_n]^\top \in \mathbb{R}^{n\times a}$ as the node features matrix. Let $\boldsymbol{z} \in \mathbb{R}^d$ be the d-dimensional graph-level representation of G, $\boldsymbol{h}_v \in \mathbb{R}^d$ be the d-dimensional node-level representation of node v, and $\boldsymbol{H} = [\boldsymbol{h}_1, ..., \boldsymbol{h}_n]^\top \in \mathbb{R}^{n\times d}$ be the node-level representations matrix of G. We denote (p, q) as an edge between nodes p, q and $(p, q) \in E$ if they are connected.

Let $\mathcal{G} = \{G_1, \dots G_N\}$ be a dataset of N graphs with K classes, where $G_i = (V_i, E_i)$. For G_i, we denote its number of nodes as n_i, graph-level representation as $\boldsymbol{z}_i$, the adjacency matrix as $\boldsymbol{A}_i$, the node feature matrix as $\boldsymbol{X}_i$, and node-level representation matrix as $\boldsymbol{H}_i$. The graph-level representation matrix of dataset $\mathcal{G}$ is denoted as $\boldsymbol{Z} = [\boldsymbol{z}_1, ..., \boldsymbol{z}_N]^\top \in \mathbb{R}^{N\times d}$. The set of all node-level representations is denoted as $\mathcal{H} = \{\boldsymbol{H}_1, \dots, \boldsymbol{H}_N\}$.

2.1 Lovász number

The definition of Lovász number [Lovász, 1979] is based on orthonormal representations of a graph. Therefore we first introduce the definition of orthonormal representations.

Definition 2.1 (Orthonormal representations)**.** Given a graph $G = (V, E)$ with $|V| = n$. Let

$$\mathcal{U} := \{\boldsymbol{U} \in \mathbb{R}^{d\times n} : \|\boldsymbol{u}_p\|_2 = 1, p = 1, 2, \dots, n;\ \boldsymbol{u}_p^\top \boldsymbol{u}_q = 0,\ \forall (p, q) \notin E\}, \tag{1}$$

where $\boldsymbol{u}_p$ is the p-th column of $\boldsymbol{U}$. Then every $\boldsymbol{U} \in \mathcal{U}$ is an orthonormal representation of G in $\mathbb{R}^d$.

Clearly, every graph has at least one orthonormal representation. For example, a trivial representation is that each node p is represented by the standard basis vector $\boldsymbol{e}_p$. Based on Definition 2.1, we introduce the Lovász number [Lovász, 1979] of a graph as follows.

Definition 2.2 (Lovász number)**.** The Lovász number of a graph $G = (V, E)$ is defined as

$$\vartheta(G) := \min_{\boldsymbol{c}, \boldsymbol{U}\in\mathcal{U}} \max_{p\in V} \frac{1}{(\boldsymbol{c}^\top \boldsymbol{u}_p)^2}, \tag{2}$$

where $\boldsymbol{c} \in \mathbb{R}^d$ ranges over all unit vectors. The vector $\boldsymbol{c}$ yielding the minimum for (2), denoted by $\boldsymbol{c}^*$, is called the *handle* of the representation, where the corresponding $\boldsymbol{U}$ is denoted as $\boldsymbol{U}^*$ for convenience. $\boldsymbol{U}^*$ is called the optimal representation of G in $\mathbb{R}^d$.

László Lovász provided a pentagon example, shown in Figure 1, to explain Lovász number defined by (2). The visualization of $\boldsymbol{U}^*$ and $\boldsymbol{c}^*$ of a pentagon is like an umbrella whose handle is $\boldsymbol{c}^*$ and the ribs are the five columns of $\boldsymbol{U}^*$. These five disjoint node pairs, i.e., $(\boldsymbol{u}_1^*, \boldsymbol{u}_3^*), (\boldsymbol{u}_1^*, \boldsymbol{u}_4^*), (\boldsymbol{u}_2^*, \boldsymbol{u}_4^*), (\boldsymbol{u}_2^*, \boldsymbol{u}_5^*), (\boldsymbol{u}_3^*, \boldsymbol{u}_5^*)$, are orthogonal to each other in visualization.

The Lovász number $\vartheta(G)$ is an upper bound on the Shannon capacity of a graph G and is polynomial-time computable [Grötschel *et al.*, 1981; Galli and Letchford, 2017] (e.g., using semidefinite programming (SDP)). Let $\bar{G}$ be the complement of G with its clique number $\omega(\bar{G})$ and chromatic number $\chi(\bar{G})$. The Lovász "sandwich theorem" shows that the Lovász number is bounded between the clique number and the chromatic number of $\bar{G}$, i.e., $\omega(\bar{G}) \leq \vartheta(G) \leq \chi(\bar{G})$. Although computing $\omega(\bar{G})$ and $\chi(\bar{G})$ are both NP-hard, the "sandwich theorem" allows us to estimate the clique number and the chromatic number of $\bar{G}$ using only $\vartheta(G)$. More detailed discussion can be found in [Knuth, 1993].

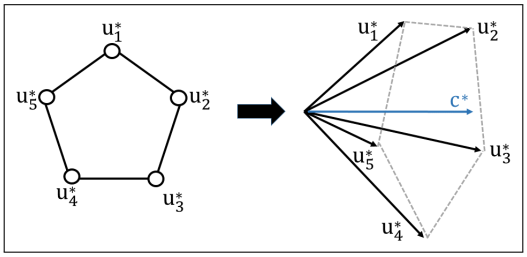

Figure 1: Pentagon example for Lovász number

2.2 Lovász theta kernel

Johansson *et al.* [2014] defined the Lovász theta kernel to evaluate the similarity between graphs. Suppose $S \subseteq V$ is a subset of the vertices of graph G, then the Lovász number of the subgraph induced by S is defined as

$$\vartheta_S(G) := \min_{\boldsymbol{c}} \max_{p \in S} \frac{1}{(\boldsymbol{c}^\top \boldsymbol{u}_p)^2}, \tag{3}$$

where $\boldsymbol{U}$ was pre-computed by Eq. (2) and $\boldsymbol{c}$ ranges over all unit vectors.

Definition 2.3 (Lovász-ϑ kernel [Johansson *et al.*, 2014])**.** Let k be a base kernel. The Lovász theta kernel between graphs $G = (V, E)$ and $G' = (V', E')$ is defined as

$$k_{\mathrm{Lo}}(G, G') = \sum_{S \subseteq V} \sum_{S' \subseteq V'} \frac{\delta(|S|, |S'|)}{C_{S,S'}} k(\vartheta_S(G), \vartheta_{S'}(G')), \tag{4}$$

where $C_{S,S'} = \binom{|V|}{|S|}\binom{|V'|}{|S'|}$, $\delta(|S|, |S'|) = 1$ if $|S| = |S'|$, and $\delta(|S|, |S'|) = 0$ otherwise.

k_{Lo} is a positive semi-definite kernel [Johansson *et al.*, 2014]. It is able to capture global properties of graphs and has been shown useful in SVM-based graph classification [Johansson *et al.*, 2014].

3 Lovász Principle for Graph Representation Learning

The Lovász number $\vartheta(G)$ of a graph G provides an insight into the global property of the graph. It is a unique and deterministic value associated with an orthonormal representation $\boldsymbol{U}^*$ and a unit *handle* vector $\boldsymbol{c}^*$. The umbrella example in Figure 1 explains how to compute the Lovász number: compacting the ribs (i.e. $\boldsymbol{U}^*$) as much as possible and using $\boldsymbol{c}^*$ as the handle. This example provides intuition that the handle vector $\boldsymbol{c}^*$ is a natural and suitable representation of the graph G.

Given $\mathcal{G} = \{G_1, G_2, \ldots, G_N\}$ drawn from an unknown distribution $\mathcal{D}_G$, we want to represent each graph as a vector such that these vectors preserve some important information of $\mathcal{D}_G$. Suppose we have an algorithm $\mathcal{A}$ such that

$$(\boldsymbol{U}_i^*, \boldsymbol{c}_i^*) = \mathcal{A}(G_i), \quad i = 1, 2, \ldots, N, \tag{5}$$

where $\mathcal{A}$ is some solver for (2). It is natural to use $\boldsymbol{c}_1^*, \boldsymbol{c}_2^*, \ldots, \boldsymbol{c}_N^*$ as representations of $G_1, G_2, \ldots, G_N$ respectively. However, this method has the following limitations[‡].

i. **Non-uniqueness** For any G_i, both $\boldsymbol{U}_i^*$ and $\boldsymbol{c}_i^*$ are not unique. For example, let $\boldsymbol{Q} \in \mathbb{R}^{d \times d}$ be an orthonormal matrix, i.e., $\boldsymbol{Q}^\top \boldsymbol{Q} = \boldsymbol{Q}\boldsymbol{Q}^\top = \boldsymbol{I}_d$, and let $\boldsymbol{c}_i' = \boldsymbol{Q}\boldsymbol{c}_i^*$ and $\boldsymbol{U}_i' = \boldsymbol{Q}\boldsymbol{U}_i^*$. We have $\|\boldsymbol{c}'\|_2 = 1$, $(\boldsymbol{U}')^\top \boldsymbol{U} = (\boldsymbol{U}_i^*)^\top \boldsymbol{U}_i^*$, and $(\boldsymbol{c}')^\top \boldsymbol{u}_p' = \vartheta(G_i)$. This means $(\boldsymbol{c}_i^*, \boldsymbol{U}_i^*)$ and $(\boldsymbol{c}_i', \boldsymbol{U}')$ yield the same Lovász number for G_i, though they could be very different. Thus, for two graphs G_i and G_j in $\mathcal{G}$, even when they are isomorphic, $\boldsymbol{c}_i^*$ and $\boldsymbol{c}_j^*$ could be very different. However, for graph representation, we hope that similar graphs have similar representations. For two graphs G_i and G_j, one may align their orthonormal representations using $\hat{\boldsymbol{Q}} = \mathrm{argmin}_{\boldsymbol{Q}^\top \boldsymbol{Q} = \boldsymbol{I}_d} \|\boldsymbol{U}_i^* - \boldsymbol{Q}\boldsymbol{U}_j^*\|_F^2$ and compare them according to $\|\boldsymbol{c}_i^* - \boldsymbol{c}_j^* \hat{\boldsymbol{Q}}\|_2$. This however only works when the $n_i = n_j$ and G_i and G_j are matched.

ii. **High computational cost** For each G_i in $\mathcal{G}$, we need to solve the optimization problem (2), for which the time complexity of SDP is at least $\mathcal{O}(|E_i| n_i^{2.5})$ [Jiang *et al.*, 2020]. Thus the total time complexity for $\mathcal{G}$ is $\mathcal{O}(\sum_{i=1}^N |E_i| n_i^{2.5})$. Therefore, this representation method is not scalable to large datasets.

iii. **Ignorance of node features** The computation of (5) solely relies on the graph structure and does not take advantage of the node feature matrix $\boldsymbol{X}_i$ that is often available and informative.

iv. **Non-generalization** Suppose we have some new graphs and want to obtain their representations. We cannot utilize the representations of $\mathcal{G}$ and we have to solve (2) again for each new graph.

v. **Non-global sensing** The computation of (5) treats each graph separately and cannot effectively take advantage of the global information or structure of $\mathcal{G}$. Individual graphs may have noise or outliers, which cannot be handled by a local method.

[‡] In our experiments (Table 1), this naive method, termed as LovászNum, is tested. In addition, the Lovász-ϑ kernel introduced in Section 2.2 is also tested.

To solve the aforementioned five issues, we present a machine learning method. We use a neural network $\mathcal{F}_W$ (parameterized by W) to approximate $\mathcal{A}$. $\mathcal{F}_W$ can be learned from $\mathcal{G}$ as well as some additional information such as the node feature matrices $\{\boldsymbol{X}_1, \ldots, \boldsymbol{X}_N\}$. Specifically, we hope that

$$(\boldsymbol{U}_i^*, \boldsymbol{c}_i^*) \approx \mathcal{F}_W(\boldsymbol{A}_i, \boldsymbol{X}_i), \quad i = 1, 2, \ldots, N. \tag{6}$$

Thus, $\mathcal{F}_W$ plays a role representing a graph (drawn from $\mathcal{D}_G$) to a matrix of nodes representation and a vector of graph representation. For new graphs sampled from $\mathcal{D}_G$, $\mathcal{F}_W$ should generalize well when the approximation errors in (6) are small enough and $\mathcal{F}_W$ is not too complex. For convenience, we split $\mathcal{F}_W$ into two parts, i.e., $\mathcal{F}_W(\cdot,\cdot) = (F(\cdot,\cdot;\theta), f(\cdot,\cdot;\phi))$, though F and f can share some parameters. We let $\boldsymbol{U}_i^* \approx F(\boldsymbol{A}_i, \boldsymbol{X}_i; \theta)$ and $\boldsymbol{c}_i^* \approx f(\boldsymbol{A}_i, \boldsymbol{X}_i; \phi)$. $F(\cdot,\cdot;\theta)$ is the model of node-level representation learning while $f(\cdot,\cdot;\phi)$ is the model of graph-level representation learning. We let

$$\boldsymbol{H}_i^\theta := F(\boldsymbol{A}_i, \boldsymbol{X}_i; \theta), \text{ and } \boldsymbol{z}_i^\phi := f(\boldsymbol{A}_i, \boldsymbol{X}_i; \phi), \ \forall i = 1, 2, ..., N. \tag{7}$$

We denote the graph-level representations matrix as $\boldsymbol{Z}_\phi = [\boldsymbol{z}_1^\phi, ..., \boldsymbol{z}_N^\phi]^\top$ and the node-level representations set as $\mathcal{H}_\theta = \{\boldsymbol{H}_1^\theta, ..., \boldsymbol{H}_N^\theta\}$. To achieve (6), we propose to solve

$$\underset{\phi,\theta}{\text{minimize}} \sum_{i=1}^{N} \left\{ \underbrace{\max_{p \in V_i} \frac{1}{\left((\boldsymbol{z}_i^\phi)^\top \boldsymbol{h}_p^\theta\right)^2}}_{\ell_1} + \mu \left(\underbrace{\left\| \boldsymbol{M}_i \odot \left(\boldsymbol{H}_i^\theta (\boldsymbol{H}_i^\theta)^\top - \boldsymbol{I}_{n_i}\right) \right\|_F^2}_{\ell_2} + \underbrace{\left((\boldsymbol{z}_i^\phi)^\top \boldsymbol{z}_i^\phi - 1\right)^2}_{\ell_3} \right) \right\}, \tag{8}$$

where $\boldsymbol{M}_i = \boldsymbol{1}_{n_i \times n_i} - \boldsymbol{A}_i$ is a mask matrix and $\mu > 0$ is a regularization parameter. The roles of ℓ_1, ℓ_2, and ℓ_3 in (8) are explained as follows.

- ℓ_1 corresponds to the objective in the definition of Lovász number of G_i.
- ℓ_2 is to approximate the orthonormal representation for G_i, i.e., $(\boldsymbol{h}_p^\theta)^\top \boldsymbol{h}_q^\theta \approx 0$ if $(p, q) \notin E_i$ and $\|\boldsymbol{h}_p\|_2 \approx 1 \ \forall p \in V_i$.
- ℓ_3 corresponds to the unit-length requirement for the handle vector of G_i, i.e., $\|\boldsymbol{z}_i^\phi\|_2 \approx 1$.

We call (8) **Lovász principle**[§], since it aims to learn an $\mathcal{F}_W$ to solve the optimization of Lovász number for the graphs drawn from $\mathcal{D}_G$. It is known that the Lovász number $\vartheta(G)$ is an upper bound on the Shannon capacity of $G = (V, E)$. The Shannon capacity [Shannon, 1956] models the amount of information that can be transmitted across a noisy communication channel, where certain signal values can be confused with each other. Here, one signal value corresponds to one node of G and $(p, q) \in E$ means that the corresponding two signals can be confused with each other. Therefore, the graph-level and node-level representations given by our Lovász principle correspond to the upper bound of the amount of information transmitted over the graph that is distinguishable between nodes.

Note that instead of the regularized unconstrained optimization (8), we can also use constrained optimization ($\ell_2 = \ell_3 = 0$), which we call strict Lovász principle. We may use the Lagrange multipliers method, projected gradient descent, or exact (or inexact) penalty method to solve the constrained optimization. Take the inexact penalty method as an example, we just need to increase the μ in (8) gradually in the optimization. The graph representation performance comparison between unconstrained and constrained optimizations will be shown in Section 6.5 and Appendix E.

For convenience, we let

$$\mathcal{L}_{\text{Lo}} := \sum_{i=1}^{|\mathcal{G}|} \max_{p \in V_i} \frac{1}{((\boldsymbol{z}_i^\phi)^\top \boldsymbol{h}_p^\theta)^2} + \mu \left(\left\| \boldsymbol{M}_i \odot \left(\boldsymbol{H}_i^\theta (\boldsymbol{H}_i^\theta)^\top - \boldsymbol{I}_{n_i}\right) \right\|_F^2 + \left((\boldsymbol{z}_i^\phi)^\top \boldsymbol{z}_i^\phi - 1\right)^2 \right), \tag{9}$$

and call it Lovász loss. The Lovász loss is mainly designed for unsupervised graph-level representation learning [Wu *et al.*, 2022; Maron *et al.*, 2019; Oono and Suzuki, 2019; Ståhlberg *et al.*, 2022], which can be used as an alternative to the popular InfoMax loss [Linsker, 1988] (see (16)).

Lovász principle for semi-supervised learning Inspired by InfoGraph [Sun *et al.*, 2019] (see (17)), we propose a Lovász loss function for semi-supervised learning tasks. Suppose the dataset $\mathcal{G}$ has

[§] We also provide an equivalent formulation based on the complement graph of G in Appendix A.

two subsets: a labeled dataset $\mathcal{G}^L$ and an unlabeled dataset $\mathcal{G}^U$. Then we deploy another supervised encoder with parameter ψ and generate the supervised node-level representations $\boldsymbol{H}_i^{\psi}$, graph-level representations $\boldsymbol{z}_i^{\psi}$, and then prediction $\hat{\boldsymbol{y}}_i^{\psi}$. The overall loss function is

$$\mathcal{L}_{\text{Lo-semi}} := \sum_{l=1}^{|\mathcal{G}^L|} \ell_{\text{supervised}}(\hat{\boldsymbol{y}}_l^{\psi}, \boldsymbol{y}_l) + \mathcal{L}_{\text{unsupervised}}(\mathcal{G}) + \lambda \sum_{i=1}^{|\mathcal{G}|} \left\| \boldsymbol{z}_i^{\phi} - \boldsymbol{z}_i^{\psi} \right\|_2^2, \tag{10}$$

where λ is a positive hyperparameter, the supervised loss $\ell_{\text{supervised}}$ is the cross-entropy loss, and the unsupervised loss $\mathcal{L}_{\text{unsupervised}}$ is the Lovász loss $\mathcal{L}_{\text{Lo}}$ (Eq. (9)) or the enhanced Lovász loss $\mathcal{L}_{\text{ELo}}$ (Eq. (14)). The last term encourages the representations learned by the two encoders to be similar.

4 Enhancing Lovász Principle with Subgraph Lovász Number

Lovász principle does not explicitly utilize the Lovász number in graph embedding, though the Lovász numbers of subgraphs can be useful in comparing graphs [Johansson *et al.*, 2014]. Therefore, we propose to use subgraph Lovász number to enhance Lovász principle based graph representation learning. We may consider taking advantage of the Lovász-ϑ kernel proposed by [Johansson *et al.*, 2014]. However, we encounter the following two difficulties.

i. Computing the Lovász numbers (3) of subgraphs is time-consuming because we need to solve (2) for every graph and the number of subgraphs of each graph is often very large (up to $2^{|V|}$). Hence, for large graph dataset, we cannot use (4) directly.

ii. The Lovász-ϑ kernel (4) is a pair-wise method and cannot effectively exploit the global structure of $\mathcal{G}$.

To solve the aforementioned problems, we present an iterative-refinement strategy that computes the subgraph Lovász numbers using the embeddings given by the Lovász principle. Specifically, at iteration t, we have the graph-level representations $\boldsymbol{Z}_{\phi}^{(t-1)}$ and the node-level representations $\mathcal{H}_{\theta}^{(t-1)}$ given by iteration $t-1$. Inspired by the Lovász-ϑ kernel (4), we compute the similarity between graph G_i and G_j as

$$K_{ij}^{(t-1)} = \sum_{S_i \subseteq V_i} \sum_{S_j \subseteq V_j} \frac{\delta(|S_i|, |S_j|)}{C_{S_i,S_j}} k(\vartheta_{S_i}^{(t-1)}(G_i), \vartheta_{S_j}^{(t-1)}(G_j)), \tag{11}$$

where $C_{S_i,S_j} = \binom{|V_i|}{|S_i|}\binom{|V_j|}{|S_j|}$ and $\vartheta_{S_i}^{(t-1)}(G_i)$ (similar for G_j) is obtained by

$$\vartheta_{S_i}^{(t-1)}(G_i) = \max_{p \in S_i} \frac{1}{(\boldsymbol{z}_i^{(t-1)\top} \boldsymbol{h}_p^{(t-1)})^2}. \tag{12}$$

The computation of $1/(\boldsymbol{z}_i^{(t-1)\top} \boldsymbol{h}_p^{(t-1)})^2$ for every $p \in V_i$ was already done when computing $\mathcal{L}_{\text{Lo}}$ via (9) at iteration $t-1$ and there is no need to solve (3). For (11), we do not need to consider all possible subgraphs and we can just randomly sample subgraphs with some fixed sizes (numbers of nodes), which is similar to the truncated Lovász-ϑ kernel of [Johansson *et al.*, 2014]. Thus we can obtain the similarity $K_{ij}^{(t-1)}$ efficiently. Adapting the idea of spectral embedding [Belkin and Niyogi, 2001], we propose the following subgraph Lovász number (SLN) loss (at iteration t)

$$\mathcal{L}_{\text{SLN}}^{(t)} := \sum_{i=1}^{|\mathcal{G}|} \sum_{j=1}^{|\mathcal{G}|} K_{ij}^{(t-1)} \left\| \boldsymbol{z}_i^{\phi} - \boldsymbol{z}_j^{\phi} \right\|_2^2 + \gamma \left(\left\| \boldsymbol{Z}_{\phi}^{\top} \boldsymbol{Z}_{\phi} - \boldsymbol{I}_d \right\|_F^2 + \left\| \boldsymbol{Z}_{\phi}^{\top} \mathbf{1}_{N \times 1} \right\|_2^2 \right), \tag{13}$$

where $\gamma > 0$. The two regularization terms in $\mathcal{L}_{\text{SLN}}^{(t)}$ aim to make the graph-level representations orthonormal and centered, which is consistent with the constraints in spectral embedding. Minimizing $\mathcal{L}_{\text{SLN}}^{(t)}$ encourages that the graph-level representations of similar graphs (in the sense of subgraph Lovász numbers) are closer to each other at iteration t. Integrating (13) with (9), we obtain the following enhanced Lovász loss at iteration t

$$\mathcal{L}_{\text{ELo}}^{(t)} := \mathcal{L}_{\text{Lo}}^{(t)} + \eta \mathcal{L}_{\text{SLN}}^{(t)}, \tag{14}$$

where $\eta > 0$ is a hyperparameter. It is worth noting that $\mathcal{L}_{\text{ELo}}$ as well as $\mathcal{L}_{\text{Lo}}$ can be implemented batch-wisely, via replacing $\mathcal{G}$ with its subsets. Similar to $\mathcal{L}_{\text{Lo}}$, $\mathcal{L}_{\text{ELo}}$ can also be applied to semi-supervised graph classification, i.e., (10).

5 Related Work

Besides the Lovász-ϑ introduced in Section 2.2, the closest work to our Lovász principle is the InfoMax principle. Following [Nowozin *et al.*, 2016; Sun *et al.*, 2019; Belghazi *et al.*, 2018], suppose the node-level representation $\boldsymbol{h}_p(x)$ and the graph-level representation $\boldsymbol{z}(x)$ are depending on the input x, T_φ is a discriminator parameterized by a neural network with parameters φ, the Jensen-Shannon mutual information (MI) estimator [Fuglede and Topsoe, 2004; Nowozin *et al.*, 2016; Hjelm *et al.*, 2019; Sun *et al.*, 2019] I_φ between $\boldsymbol{h}_p$ and $\boldsymbol{z}$ is defined as

$$I_\varphi(\boldsymbol{h}_p, \boldsymbol{z}) = \mathbb{E}_{\mathbb{P}}[-\mathrm{sp}(-T_\varphi(\boldsymbol{h}_p(x), \boldsymbol{z}(x)))] - \mathbb{E}_{\mathbb{P}\times\tilde{\mathbb{P}}}[\mathrm{sp}(T_\varphi(\boldsymbol{h}_p(x'), \boldsymbol{z}(x)))], \tag{15}$$

where x is the input sample from distribution $\mathbb{P}$, x' is the negative sample from distribution $\tilde{\mathbb{P}}$, and $\mathrm{sp}(a) = \log(1 + e^a)$ denotes the softplus function. Many recent graph-level representation learning methods [Sun *et al.*, 2019; You *et al.*, 2020; Yin *et al.*, 2022] are based on the InfoMax principle, i.e., maximizing (15). For instance, the InfoGraph proposed by [Sun *et al.*, 2019] obtains graph-level representations by maximizing the mutual information between the graph-level representation and the node-level representations as follows

$$\phi^*, \theta^*, \varphi^* = \underset{\phi,\theta,\varphi}{\arg\max} \sum_{i=1}^{|\mathcal{G}|} \frac{1}{|V_i|} \sum_{p\in V_i} I_\varphi(\boldsymbol{h}_p^\theta, \boldsymbol{z}_i^\phi) \triangleq -\mathcal{L}_{\text{unsupervised}}^{I_\varphi}(\mathcal{G}). \tag{16}$$

For semi-supervised learning, the dataset $\mathcal{G}$ is split into labeled dataset $\mathcal{G}^L$ and unlabeled dataset $\mathcal{G}^U$. They deploy another supervised encoder with parameter ψ and then generate the supervised node-level representations $\boldsymbol{H}_i^\psi$, graph-level representations $\boldsymbol{z}_i^\psi$ and prediction $\hat{\boldsymbol{y}}_i^\psi$. The loss function of InfoGraph for semi-supervised learning is defined as follows

$$\mathcal{L}_{\text{info-semi}} = \sum_{l=1}^{|\mathcal{G}^L|} \ell_{\text{supervised}}(\hat{\boldsymbol{y}}_l^\psi, \boldsymbol{y}_l) + \mathcal{L}_{\text{unsupervised}}^{I_\varphi}(\mathcal{G}) - \lambda \sum_{i=1}^{|\mathcal{G}|} \frac{1}{|V_i|} I_\varphi(\boldsymbol{z}_i^\phi . \boldsymbol{z}_i^\psi). \tag{17}$$

The comparison between the InfoMax principle and our Lovász principle is as follows.

- The InfoMax principle focuses on the mutual information between graph-level representation and node-level representation, while our Lovász principle is derived from the Lovász number, a fundamental topological property of graph.
- Our Lovász principle only needs to optimize ϕ and θ. Differently, besides ϕ and θ, the InfoMax principle has to optimize an additional discriminator parameter φ for the Jensen-Shannon MI estimator. Thus, our Lovász principle is simpler than the InfoMax principle.
- Approximating mutual information using neural network is challenging [Nowozin *et al.*, 2016] and the Jensen-Shannon MI estimator I_φ only provides an approximation by sampling rather than an exact computation. In contrast, our Lovász principle does not rely on mutual information and sampling.

It is worth noting that the Lovász convolutional networks (LCN) proposed by [Yadav *et al.*, 2019] was motivated by the observation that removing certain vertices from a graph doesn't affect the graph's global properties such as the Lovász number. LCN does not involve any optimization related to the Lovász number and was designed as an alternative to GCN. Our Lovász principle is an optimization principle that can be used in any graph neural network (e.g. LCN). It is also useful in many applications such as graph prompt learning [Liu *et al.*, 2023; Sun *et al.*, 2022] and graph anomaly detection [Ma *et al.*, 2021; Zhang *et al.*, 2023; Cai *et al.*, 2023].

6 Experiments

In this section, we evaluate the effectiveness of the Lovász principle compared to the InfoMax principle in graph representation learning methods and a few other baselines such as graph kernels. The graph representation learning methods we considered in this paper include InfoGraph [Sun *et al.*, 2019], GraphCL [You *et al.*, 2020], AD-GCL [Suresh *et al.*, 2021], JOAO [You *et al.*, 2021], and AutoGCL [Yin *et al.*, 2022], which are the most current and influential methods spanning from

2019 to 2022. Note that the graph-level representation learning principles (GIB) [Wu *et al.*, 2020] and (SIB) [Yu *et al.*, 2021] are not suitable for unsupervised graph learning and hence will not be compared in this work. To ensure fair comparisons, we follow the neural network architectures of those InfoMax based methods and replace the InfoMax loss (Eq. (16)) with the Lovász loss $\mathcal{L}_{\mathrm{Lo}}$ (Eq. (9)) or enhanced Lovász loss $\mathcal{L}_{\mathrm{ELo}}$ (Eq. (14)) while keeping the network structures and parameter settings unchanged. We conduct the experiments on TUD benchmark datasets [Morris *et al.*, 2020] and ChEMBL benchmark datasets [Mayr *et al.*, 2018; Gaulton *et al.*, 2012].

6.1 Unsupervised Learning

The first category of compare methods is graph kernel-based methods such as graphlet kernel (GL) [Shervashidze *et al.*, 2009], Weisfeiler-Lehman sub-tree kernel (WL) [Shervashidze *et al.*, 2011], deep graph kernel (DGK) [Yanardag and Vishwanathan, 2015], and Lovász-ϑ kernel [Johansson *et al.*, 2014]. The second category is traditional unsupervised graph representation methods like node2vec [Grover and Leskovec, 2016], sub2vec Adhikari *et al.* [2018], and graph2vec [Narayanan *et al.*, 2017]. The third category is the methods based on the InfoMax principle (Eq. (16)), including InfoGraph [Sun *et al.*, 2019], GraphCL [You *et al.*, 2020], AD-GCL [Suresh *et al.*, 2021], JOAOv2 [You *et al.*, 2021], and AutoGCL [Yin *et al.*, 2022]. We also include the Lovász number method (LovászNum) [Lovász, 1979] as a baseline, where we solve the Lovász number (Eq. (2)) using semidefinite programming (SDP) [Wolkowicz *et al.*, 2012] and then use the handle vector $\boldsymbol{c}^*$ as the graph-level representation.

Following [Sun *et al.*, 2019; You *et al.*, 2021; Yin *et al.*, 2022], we train a graph representation model on unlabeled data to obtain graph representations and use these representations and graph labels to train a classifier. Our experimental setup is similar to that of AutoGCL [Yin *et al.*, 2022]. Specifically, we use a 5-layer GIN [Xu *et al.*, 2018] with hidden size 128 as the representation model and an SVM as the classifier. The model is trained with a batch size of 128 and a learning rate of 0.001. For those contrastive learning methods (e.g., JOJOv2 and AutoGCL), we use 30 epochs of contrastive pre-training under the naive strategy. We perform 10-fold cross-validation on each dataset and repeat 10 times with different random seeds and record the average accuracy (ACC) and standard deviation.

Table 1: Performance (ACC) of unsupervised learning. The baseline results are from AutoGCL [Yin *et al.*, 2022] and JOAO [You *et al.*, 2021]. The **bold**, blue and green numbers denote the best, second best and third best performances respectively, which also applies to Tables 2 and 3.

	methods	MUTAG	PROTEINS	DD	NCI1	COLLAB	IMDB-B	REDDIT-B	REDDIT-M5K
kernels	GL	81.66±2.11	-	-	-	-	65.87±0.98	77.34±0.18	41.01± 0.17
	WL	80.72±3.00	72.92±0.56	-	80.01±0.50	-	72.30±3.44	68.82±0.41	46.06± 0.21
	DGK	87.44±2.72	73.30±0.82	-	80.31±0.46	-	66.96±0.56	78.04±0.39	41.27±0.18
	Lovász-ϑ	82.57±1.68	71.86±1.41	-	75.90±1.33	-	67.26±1.85	76.03±1.87	43.57±1.79
vector embedding	node2vec	72.63±10.20	57.49±3.57	-	54.89±1.61	-	-	-	-
	sub2vec	61.05±15.80	53.03±5.55	-	52.84±1.47	-	55.26±1.54	71.48±0.41	36.68±0.42
	graph2vec	83.15±9.25	73.30±2.05	-	73.22±1.81	-	71.10±0.54	75.78±1.03	47.86±0.26
InfoMax principle	InfoGraph	89.01±1.13	74.44±0.31	72.85±1.78	76.20±1.06	70.65±1.13	73.03±0.87	82.50±1.42	53.46±1.03
	GraphCL	86.80±1.34	74.39±0.45	78.62±0.40	77.87±0.41	71.36±1.15	71.14±0.44	89.53±0.84	55.99±0.28
	AD-GCL	87.13±1.56	73.59±0.65	74.49±0.52	69.67±0.51	73.32±0.61	71.57±1.01	85.52±0.79	53.00±0.82
	JOAOv2	86.91±1.01	71.25±0.85	66.91±1.75	72.99±0.75	70.40±2.21	71.60±0.86	78.35±1.38	55.57±2.86
	AutoGCL	88.64±1.08	75.80±0.36	77.57±0.60	82.00±0.29	70.12±0.68	73.30±0.40	88.58±1.49	56.75±0.18
	LovászNum	81.24±1.59	62.46±1.31	67.65±2.31	74.73±1.88	72.47±1.83	70.57±1.73	71.25±1.59	43.24±1.72
Lovász principle (use $\mathcal{L}_{\mathrm{Lo}}$)	InfoGraph	89.67±1.54	75.26±1.43	74.13±1.49	78.21±1.35	71.46±1.21	73.87±1.32	84.76±1.86	54.57±1.38
	GraphCL	87.24±1.96	75.87±2.17	79.14±1.67	79.13±1.27	72.52±1.37	72.44±1.46	89.87±2.13	56.12±1.73
	AD-GCL	87.44±2.13	74.29±2.80	76.25±1.48	75.12±2.13	73.85±1.05	73.02±1.35	87.11±1.95	54.61±2.35
	JOAOv2	87.19±1.92	73.15±1.46	73.15±2.17	74.15±1.67	72.62±1.43	72.18±1.72	84.19±1.67	53.74±1.70
	AutoGCL	89.02±1.47	76.23±1.25	78.95±1.39	82.63±2.12	71.31±1.72	73.95±1.36	89.41±1.81	57.28±1.62
Lovász principle (use $\mathcal{L}_{\mathrm{ELo}}$)	InfoGraph	**90.13±2.05**	76.12±1.72	75.76±1.64	79.36±1.57	72.67±1.95	**74.96±1.49**	84.53±1.79	55.12±1.47
	GraphCL	87.93±2.42	**76.82±1.34**	77.35±1.95	80.11±1.47	74.16±1.37	73.87±1.52	90.23±1.87	56.83±1.35
	AD-GCL	88.50±1.82	75.22±1.93	76.14±1.21	78.15±1.81	**74.57±1.98**	73.48±1.41	88.16±1.37	55.64±1.63
	JOAOv2	88.76±1.43	75.27±1.61	74.62±2.58	76.23±1.75	72.85±1.73	72.97±1.37	85.31±1.48	54.68±1.48
	AutoGCL	89.87±1.85	76.03±1.37	**79.31±1.27**	**82.95±1.26**	72.23±1.52	74.52±1.44	**90.65±1.46**	**57.93±1.72**

As shown in Table 1, the enhanced Lovász loss $\mathcal{L}_{\mathrm{ELo}}$ (Eq. (14)) achieves the best performance on all datasets. By replacing the InfoMax loss with the Lovász loss $\mathcal{L}_{\mathrm{Lo}}$, the performances of the five graph representation learning methods are improved, which demonstrates the effectiveness of the Lovász principle. Furthermore, $\mathcal{L}_{\mathrm{ELo}}$ outperformed $\mathcal{L}_{\mathrm{Lo}}$ in most cases, which verified the effectiveness of introducing subgraph Lovász numbers to the Lovász principle. It is worth noting that the LovászNum method performs worse than the Lovász principle based methods, which confirms the limitations we analyzed in Section 3 and verifies the necessity and significance of our proposed methods.

6.2 Semi-supervised Learning

Following [Hu *et al.*, 2019; You *et al.*, 2021; Yin *et al.*, 2022], we compare Lovász principle with InfoMax principle in semi-supervised learning tasks. The semi-supervised losses of our Lovász principle based methods and InfoMax based methods $\mathcal{L}_{\text{info-semi}}$ were shown in (10) and (17) respectively. Following the settings of AutoGCL [Yin *et al.*, 2022], we employ a 10-fold cross-validation on each dataset. For each fold, we use 80% of the total data as the unlabeled data, 10% as labeled training data, and 10% as labeled testing data. The classifier for labeled data is a ResGCN [Chen *et al.*, 2019] with 5 layers and a hidden size of 128. We repeat each experiment 10 times and report the average accuracy in Table 2. We see that our Lovász loss $\mathcal{L}_{\text{Lo}}$ and the enhanced Lovász loss $\mathcal{L}_{\text{ELo}}$ outperformed InfoMax loss in all cases. Furthermore, $\mathcal{L}_{\text{ELo}}$ outperformed $\mathcal{L}_{\text{Lo}}$ in most cases. These results are consistent with those in Secion 6.1.

Table 2: Performance (ACC) of semi-supervised learning.

	methods	NCI1	PROTEINS	DD	COLLAB	REDDIT-B	REDDIT-M5K	GITHUB
	no Pretrain	73.72±0.24	70.40±1.54	73.56±0.41	73.71±0.27	86.63±0.27	51.33±0.44	60.87±0.17
Pretrain-GNN	Infomax	74.86±0.26	72.27±0.40	75.78±0.34	73.76±0.29	88.66±0.95	53.61±0.31	65.21±0.88
	ContextPred	73.00±0.30	70.23±0.63	74.66±0.51	73.69±0.37	84.76±0.52	51.23±0.84	62.35±0.73
InfoMax principle	GraphCL	74.63±0.25	74.17±0.34	76.17±1.37	74.23±0.21	89.11±0.19	52.55±0.45	65.81±0.79
	AD-GCL	75.18±0.31	73.96±0.47	77.91±0.73	75.82±0.26	90.10±0.15	53.49±0.28	64.17±1.38
	JOAOv2	74.86±0.39	73.31±0.48	75.81±0.73	75.53±0.18	88.79±0.65	52.71±0.28	66.66±0.60
	AutoGCL	73.75±2.25	75.65±2.40	77.50±4.41	77.16±1.48	79.80±3.47	49.91±2.70	62.46±1.51
Lovász principle (use $\mathcal{L}_{\text{Lo}}$)	GraphCL	75.46±1.53	75.12±1.87	77.46±1.52	76.12±1.15	89.87±1.68	53.69±1.68	66.72±1.53
	AD-GCL	76.62±1.83	74.21±1.71	78.27±1.39	76.27±1.74	90.36±1.56	54.06±1.32	65.32±1.04
	JOAOv2	76.13±1.76	73.73±1.86	76.27±1.48	77.35±1.27	89.31±1.85	53.17±1.76	66.35±1.96
	AutoGCL	75.77±1.48	76.36±1.57	78.16±1.61	77.63±1.78	84.64±2.53	51.31±1.81	64.87±1.62
Lovász principle (use $\mathcal{L}_{\text{ELo}}$)	GraphCL	75.81±1.68	75.88±1.67	78.43±1.48	77.57±1.58	90.67±1.27	54.81±1.73	67.04±1.45
	AD-GCL	**77.28±1.04**	75.43±1.58	78.67±1.64	76.98±1.87	**91.54±1.39**	**55.46±1.59**	66.87±1.25
	JOAOv2	76.25±1.59	74.67±1.37	77.96±1.86	**78.84±1.75**	90.25±1.22	54.32±1.89	**67.52±1.73**
	AutoGCL	76.53±1.92	**76.89±1.55**	**78.82±1.90**	78.46±1.39	87.31±1.57	53.17±1.50	66.47±1.26

6.3 Transfer Learning

Following [Hu *et al.*, 2019; You *et al.*, 2021; Yin *et al.*, 2022], we compare the performance of our Lovász principles with the InfoMax principle in the task of transfer learning. We use the Pretrain-GNN method [Hu *et al.*, 2019] as a baseline and employ the Infomax, EdgePred, AttrMasking, and ContextPred pre-training strategies. The experimental settings follow those of AutoGCL [Yin *et al.*, 2022]. More details are in the appendix. As shown in Table 3, the improved Lovász loss $\mathcal{L}_{\text{ELo}}$ performs the best on transfer learning tasks. In addition, the Lovász principle based methods generally outperform those based on the InfoMax principle in most cases.

Table 3: Performance (ROC-AUC score) of transfer learning.

	methods	BBBP	Tox21	ToxCast	SIDER	ClinTox	MUV	HIV	BACE
	no Pretrain	65.8±4.5	74.0±0.8	63.4±0.6	57.3±1.6	58.0±4.4	71.8±2.5	75.3±1.9	70.1±5.4
Pretrain-GNN's strategies	Infomax	68.8±0.8	75.3±0.5	62.7±0.4	58.4±0.8	69.9±3.0	75.3±2.5	76.0±0.7	75.9±1.6
	EdgePred	67.3±2.4	76.0±0.6	64.1±0.6	60.4±0.7	64.1±3.7	74.1±2.1	76.3±1.0	79.9±0.9
	AttrMasking	64.3±2.8	76.7±0.4	64.2±0.5	61.0±0.7	71.8±4.1	74.7±1.4	77.2±1.1	79.3±1.6
	ContextPred	68.0±2.0	75.7±0.7	63.9±0.6	60.9±0.6	65.9±3.8	75.8±1.7	77.3±1.0	79.6±1.2
InfoMax principle	GraphCL	69.68±0.67	73.87±0.66	62.40±0.57	60.53±0.88	75.99±2.65	69.80±2.66	78.47±1.22	75.38±1.44
	AD-GCL	70.01±1.07	76.54±0.82	63.07±0.72	63.28±0.79	79.78±3.52	72.30±1.61	78.28±0.97	78.51±0.80
	JOAOv2	71.39±0.92	74.27±0.62	63.16±0.45	60.49±0.74	80.97±1.64	73.67±1.00	77.51±1.17	75.49±1.27
	AutoGCL	73.36±0.77	75.69±0.29	63.47±0.38	62.51±0.63	80.99±3.38	75.83±1.30	78.35±0.64	83.26±1.13
Lovász principle (use $\mathcal{L}_{\text{Lo}}$)	GraphCL	71.37±1.74	75.66±1.82	63.35±1.47	62.11±1.35	77.02±1.67	72.25±1.42	79.23±1.43	78.51±1.58
	AD-GCL	72.24±1.89	77.52±1.74	63.56±1.36	63.87±1.53	80.35±2.36	74.42±1.57	78.95±2.21	80.17±1.04
	JOAOv2	72.16±1.35	75.86±1.21	63.92±1.52	62.56±1.12	81.26±2.37	75.94±1.38	79.01±2.68	79.82±1.39
	AutoGCL	73.79±1.41	76.13±1.48	64.21±1.58	63.24±1.51	81.32±2.12	76.04±1.87	78.64±1.95	82.57±1.95
Lovász principle (use $\mathcal{L}_{\text{ELo}}$)	GraphCL	73.05±1.21	76.45±1.35	64.58±1.73	63.72±1.52	80.21±2.31	74.43±1.95	80.37±1.52	80.63±1.63
	AD-GCL	72.48±1.59	**77.96±1.71**	64.27±1.68	63.91±1.74	81.76±2.01	75.88±1.48	**81.08±2.35**	82.21±1.49
	JOAOv2	74.13±1.26	76.21±1.35	64.81±1.92	63.38±1.89	**82.75±2.69**	76.51±1.53	81.13±1.96	81.34±1.35
	AutoGCL	**74.67±1.81**	76.97±1.76	**65.36±1.45**	**64.13±1.48**	82.13±2.41	**76.93±1.62**	79.56±1.41	**83.57±1.30**

6.4 Overall Performance and Significance Analysis

For convenience, we show the average performance of all methods over all datasets in Figure 2. We see our Lovász principles outperformed other methods in the three tasks.

To measure the significance of the improvement over the baselines, we implement paired t-tests on the mean scores obtained from the datasets. A p-value below 0.05 indicates a significant difference. The results presented in Table 4 demonstrate the statistical significance of the improvements achieved by our methods across all the datasets.

https://doi.org/10.52202/075280-2540

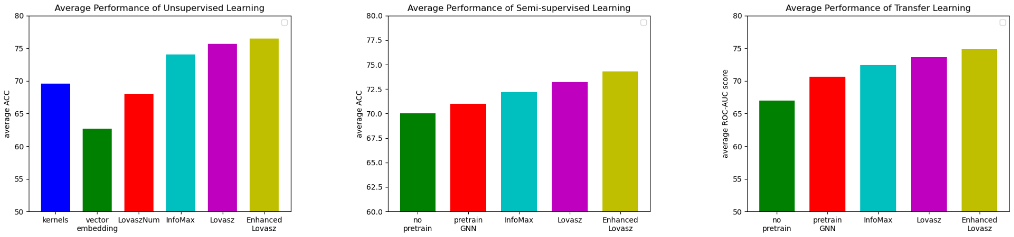

(a) Unsupervised learning (b) Semi-supervised learning (c) Transfer learning

Figure 2: The average performance of different types of methods

Table 4: Significance analysis (p-values) of improvement via the paired t-test. A p-value less than 0.05 indicates a significant improvement.

tasks	principles comparison	InfoGraph	GraphCL	AD-GCL	JOAOv2	AutoGCL
unsupervised	InfoMax vs Lovász ($\mathcal{L}_{\mathrm{Lo}}$)	0.00067	0.00286	0.02238	0.07347	0.00059
	InfoMax vs Lovász ($\mathcal{L}_{\mathrm{ELo}}$)	0.00005	0.01626	0.01541	0.01319	0.00035
	Lovász ($\mathcal{L}_{\mathrm{Lo}}$) vs Lovász ($\mathcal{L}_{\mathrm{ELo}}$)	0.00429	0.10925	0.01522	0.00079	0.00466
semi-supervised	InfoMax vs Lovász ($\mathcal{L}_{\mathrm{Lo}}$)	-	0.00028	0.01115	0.04290	0.02147
	InfoMax vs Lovász ($\mathcal{L}_{\mathrm{ELo}}$)	-	0.00051	0.00051	0.00116	0.01129
	Lovász ($\mathcal{L}_{\mathrm{Lo}}$) vs Lovász ($\mathcal{L}_{\mathrm{ELo}}$)	-	0.00169	0.00076	0.00133	0.00545

6.5 Measuring the Quality of Solver Approximation

Given a GNN model $\mathcal{F}_W$ trained via the Lovász principle, the predicted Lovász number of a graph G is denoted as $\hat{\vartheta}(G)$, while the ground-truth Lovász number $\vartheta(G)$ can be computed by SDP [Wolkowicz *et al.*, 2012]. Then we define the relative prediction error for the Lovász number as

$$e_\vartheta = |\hat{\vartheta}(G) - \vartheta(G)|/\vartheta(G). \tag{18}$$

Besides the regularized optimization of the Lovász principle in (9), we also propose a constrained optimization method in Appendix E. We select 50 graphs from each of the four datasets and report e_ϑ given by both the regularized ($\mu = 10$) optimization and the constrained optimization for Lovász principle in Table 5. We can see that in almost all cases, the relative prediction errors are less than 10%. This indicates that the $\mathcal{F}_W$ trained by the Lovász principle is a good and reliable approximator for the solver $\mathcal{A}$ of the Lovász number. This is similar to the idea of learning to optimize.

Table 5: Relative prediction errors e_ϑ given by regularized optimization and constrained optimization

e_ϑ (%)	MUTAG	PROTEINS	DD	NCI1
regularized optimization	9.7± 3.4	8.2±2.1	6.3±1.1	10.2± 3.6
constrained optimization	6.5± 2.4	7.3±1.6	6.1±1.2	8.5± 2.3

6.6 More Numerical Results

The results of **parameter sensitivity analysis**, **ablation study**, and **time cost comparison** are in Appendix C, Appendix D, and Appendix F respectively.

7 Conclusions

This paper proposed a novel method called Lovász principle for unsupervised graph-level representation learning. An extension using the subgraph Lovász number was also presented. The numerical results of unsupervised learning, semi-supervised learning, and transfer learning showed that the proposed methods are more effective than graph kernels and InfoMax principle based representation learning methods. Besides unsupervised representation learning, it is possible to apply our methods to other tasks such as graph-level clustering and graph generation. For instance, we can add a clustering module (e.g. [Xie *et al.*, 2016]) to $\mathcal{L}_{\mathrm{Lo}}$ to construct an end-to-end clustering algorithm. We can combine $\mathcal{L}_{\mathrm{Lo}}$ with variational autoencoder [Kingma and Welling, 2013] to train a model to generate new graphs. Nevertheless, the implementation of these methods is out of the scope of this paper.

Acknowledgments

This work was partially supported by the Youth program 62106211 of the National Natural Science Foundation of China, the General Program JCYJ20210324130208022 of Shenzhen Fundamental Research, the research funding T00120210002 of Shenzhen Research Institute of Big Data, the Guangdong Key Lab of Mathematical Foundations for Artificial Intelligence, and the funding UDF01001770 of The Chinese University of Hong Kong, Shenzhen.

The authors appreciate the reviewers' and AC's comments and time.

References

Bijaya Adhikari, Yao Zhang, Naren Ramakrishnan, and B Aditya Prakash. Sub2vec: Feature learning for subgraphs. In *Advances in Knowledge Discovery and Data Mining: 22nd Pacific-Asia Conference, PAKDD 2018, Melbourne, VIC, Australia, June 3-6, 2018, Proceedings, Part II 22*, pages 170–182. Springer, 2018.

Yunsheng Bai, Hao Ding, Yang Qiao, Agustin Marinovic, Ken Gu, Ting Chen, Yizhou Sun, and Wei Wang. Unsupervised inductive graph-level representation learning via graph-graph proximity. *arXiv preprint arXiv:1904.01098*, 2019.

Mohamed Ishmael Belghazi, Aristide Baratin, Sai Rajeshwar, Sherjil Ozair, Yoshua Bengio, Aaron Courville, and Devon Hjelm. Mutual information neural estimation. In *International conference on machine learning*, pages 531–540. PMLR, 2018.

Mikhail Belkin and Partha Niyogi. Laplacian eigenmaps and spectral techniques for embedding and clustering. *Advances in neural information processing systems*, 14, 2001.

Karsten M Borgwardt, Cheng Soon Ong, Stefan Schönauer, SVN Vishwanathan, Alex J Smola, and Hans-Peter Kriegel. Protein function prediction via graph kernels. *Bioinformatics*, 21(suppl_1):i47–i56, 2005.

Jinyu Cai, Yunhe Zhang, and Jicong Fan. Self-discriminative modeling for anomalous graph detection. *arXiv preprint arXiv:2310.06261*, 2023.

Ting Chen, Song Bian, and Yizhou Sun. Are powerful graph neural nets necessary? a dissection on graph classification. *arXiv preprint arXiv:1905.04579*, 2019.

Ganqu Cui, Jie Zhou, Cheng Yang, and Zhiyuan Liu. Adaptive graph encoder for attributed graph embedding. In *Proceedings of the 26th ACM SIGKDD International Conference on Knowledge Discovery & Data Mining*, pages 976–985, 2020.

Asim Kumar Debnath, Rosa L Lopez de Compadre, Gargi Debnath, Alan J Shusterman, and Corwin Hansch. Structure-activity relationship of mutagenic aromatic and heteroaromatic nitro compounds. correlation with molecular orbital energies and hydrophobicity. *Journal of medicinal chemistry*, 34(2):786–797, 1991.

Kaize Ding, Zhe Xu, Hanghang Tong, and Huan Liu. Data augmentation for deep graph learning: A survey. *ACM SIGKDD Explorations Newsletter*, 24(2):61–77, 2022.

Yin Fang, Qiang Zhang, Haihong Yang, Xiang Zhuang, Shumin Deng, Wen Zhang, Ming Qin, Zhuo Chen, Xiaohui Fan, and Huajun Chen. Molecular contrastive learning with chemical element knowledge graph. In *Proceedings of the AAAI Conference on Artificial Intelligence*, volume 36, pages 3968–3976, 2022.

Bent Fuglede and Flemming Topsoe. Jensen-shannon divergence and hilbert space embedding. In *International symposium onInformation theory, 2004. ISIT 2004. Proceedings.*, page 31. IEEE, 2004.

Laura Galli and Adam N. Letchford. On the lovász theta function and some variants. *Discrete Optimization*, 25:159–174, 2017.

Thomas Gärtner, Peter Flach, and Stefan Wrobel. On graph kernels: Hardness results and efficient alternatives. In *Learning theory and kernel machines*, pages 129–143. Springer, 2003.

https://doi.org/10.52202/075280-2540

Anna Gaulton, Louisa J Bellis, A Patricia Bento, Jon Chambers, Mark Davies, Anne Hersey, Yvonne Light, Shaun McGlinchey, David Michalovich, Bissan Al-Lazikani, et al. Chembl: a large-scale bioactivity database for drug discovery. *Nucleic acids research*, 40(D1):D1100–D1107, 2012.

Justin Gilmer, Samuel S Schoenholz, Patrick F Riley, Oriol Vinyals, and George E Dahl. Neural message passing for quantum chemistry. In *International conference on machine learning*, pages 1263–1272. PMLR, 2017.

Martin Grötschel, László Lovász, and Alexander Schrijver. The ellipsoid method and its consequences in combinatorial optimization. *Combinatorica*, 1:169–197, 1981.

Aditya Grover and Jure Leskovec. node2vec: Scalable feature learning for networks. In *Proceedings of the 22nd ACM SIGKDD international conference on Knowledge discovery and data mining*, pages 855–864, 2016.

William L Hamilton, Rex Ying, and Jure Leskovec. Representation learning on graphs: Methods and applications. *arXiv preprint arXiv:1709.05584*, 2017.

Xiaotian Han, Zhimeng Jiang, Ninghao Liu, and Xia Hu. G-mixup: Graph data augmentation for graph classification. In *International Conference on Machine Learning*, pages 8230–8248. PMLR, 2022.

Kaveh Hassani and Amir Hosein Khasahmadi. Contrastive multi-view representation learning on graphs. In *International conference on machine learning*, pages 4116–4126. PMLR, 2020.

R Devon Hjelm, Alex Fedorov, Samuel Lavoie-Marchildon, Karan Grewal, Phil Bachman, Adam Trischler, and Yoshua Bengio. Learning deep representations by mutual information estimation and maximization. In *International Conference on Learning Representations*, 2019.

Zhenyu Hou, Xiao Liu, Yukuo Cen, Yuxiao Dong, Hongxia Yang, Chunjie Wang, and Jie Tang. Graphmae: Self-supervised masked graph autoencoders. In *Proceedings of the 28th ACM SIGKDD Conference on Knowledge Discovery and Data Mining*, pages 594–604, 2022.

Weihua Hu, Bowen Liu, Joseph Gomes, Marinka Zitnik, Percy Liang, Vijay Pande, and Jure Leskovec. Strategies for pre-training graph neural networks. *arXiv preprint arXiv:1905.12265*, 2019.

Haotian Jiang, Tarun Kathuria, Yin Tat Lee, Swati Padmanabhan, and Zhao Song. A faster interior point method for semidefinite programming. In *2020 IEEE 61st annual symposium on foundations of computer science (FOCS)*, pages 910–918. IEEE, 2020.

Fredrik Johansson, Vinay Jethava, Devdatt Dubhashi, and Chiranjib Bhattacharyya. Global graph kernels using geometric embeddings. In *International Conference on Machine Learning*, pages 694–702. PMLR, 2014.

Diederik P Kingma and Max Welling. Auto-encoding variational bayes. *arXiv preprint arXiv:1312.6114*, 2013.

Thomas N Kipf and Max Welling. Variational graph auto-encoders. *arXiv preprint arXiv:1611.07308*, 2016.

Thomas Kipf, Ethan Fetaya, Kuan-Chieh Wang, Max Welling, and Richard Zemel. Neural relational inference for interacting systems. In *International Conference on Machine Learning*, pages 2688–2697. PMLR, 2018.

Donald E Knuth. The sandwich theorem. *arXiv preprint math/9312214*, 1993.

Nils Kriege and Petra Mutzel. Subgraph matching kernels for attributed graphs. *arXiv preprint arXiv:1206.6483*, 2012.

Phuc H Le-Khac, Graham Healy, and Alan F Smeaton. Contrastive representation learning: A framework and review. *Ieee Access*, 8:193907–193934, 2020.

Namkyeong Lee, Junseok Lee, and Chanyoung Park. Augmentation-free self-supervised learning on graphs. In *Proceedings of the AAAI Conference on Artificial Intelligence*, volume 36, pages 7372–7380, 2022.

https://doi.org/10.52202/075280-2540

Shuangli Li, Jingbo Zhou, Tong Xu, Dejing Dou, and Hui Xiong. Geomgcl: Geometric graph contrastive learning for molecular property prediction. In *Proceedings of the AAAI Conference on Artificial Intelligence*, volume 36, pages 4541–4549, 2022.

Yinqi Li, Hong Chang, Bingpeng Ma, Shiguang Shan, and Xilin Chen. Optimal positive generation via latent transformation for contrastive learning. *Advances in Neural Information Processing Systems*, 35:18327–18342, 2022.

Ralph Linsker. Self-organization in a perceptual network. *Computer*, 21(3):105–117, 1988.

Yixin Liu, Ming Jin, Shirui Pan, Chuan Zhou, Yu Zheng, Feng Xia, and S Yu Philip. Graph self-supervised learning: A survey. *IEEE Transactions on Knowledge and Data Engineering*, 35(6):5879–5900, 2022.

Zemin Liu, Xingtong Yu, Yuan Fang, and Xinming Zhang. Graphprompt: Unifying pre-training and downstream tasks for graph neural networks. In *Proceedings of the ACM Web Conference 2023*, pages 417–428, 2023.

László Lovász. On the shannon capacity of a graph. *IEEE Transactions on Information theory*, 25(1):1–7, 1979.

Xiaoxiao Ma, Jia Wu, Shan Xue, Jian Yang, Chuan Zhou, Quan Z Sheng, Hui Xiong, and Leman Akoglu. A comprehensive survey on graph anomaly detection with deep learning. *IEEE Transactions on Knowledge and Data Engineering*, 2021.

Haggai Maron, Heli Ben-Hamu, Hadar Serviansky, and Yaron Lipman. Provably powerful graph networks. *Advances in neural information processing systems*, 32, 2019.

Andreas Mayr, Günter Klambauer, Thomas Unterthiner, Marvin Steijaert, Jörg K Wegner, Hugo Ceulemans, Djork-Arné Clevert, and Sepp Hochreiter. Large-scale comparison of machine learning methods for drug target prediction on chembl. *Chemical science*, 9(24):5441–5451, 2018.

Yujie Mo, Liang Peng, Jie Xu, Xiaoshuang Shi, and Xiaofeng Zhu. Simple unsupervised graph representation learning. In *Proceedings of the AAAI Conference on Artificial Intelligence*, volume 36, pages 7797–7805, 2022.

Christopher Morris, Nils M Kriege, Franka Bause, Kristian Kersting, Petra Mutzel, and Marion Neumann. Tudataset: A collection of benchmark datasets for learning with graphs. *arXiv preprint arXiv:2007.08663*, 2020.

Annamalai Narayanan, Mahinthan Chandramohan, Rajasekar Venkatesan, Lihui Chen, Yang Liu, and Shantanu Jaiswal. graph2vec: Learning distributed representations of graphs. *arXiv preprint arXiv:1707.05005*, 2017.

Sebastian Nowozin, Botond Cseke, and Ryota Tomioka. f-gan: Training generative neural samplers using variational divergence minimization. *Advances in neural information processing systems*, 29, 2016.

Kenta Oono and Taiji Suzuki. Graph neural networks exponentially lose expressive power for node classification. *arXiv preprint arXiv:1905.10947*, 2019.

Zhen Peng, Wenbing Huang, Minnan Luo, Qinghua Zheng, Yu Rong, Tingyang Xu, and Junzhou Huang. Graph representation learning via graphical mutual information maximization. In *Proceedings of The Web Conference 2020*, pages 259–270, 2020.

Jiezhong Qiu, Qibin Chen, Yuxiao Dong, Jing Zhang, Hongxia Yang, Ming Ding, Kuansan Wang, and Jie Tang. Gcc: Graph contrastive coding for graph neural network pre-training. In *Proceedings of the 26th ACM SIGKDD international conference on knowledge discovery & data mining*, pages 1150–1160, 2020.

Yu Rong, Yatao Bian, Tingyang Xu, Weiyang Xie, Ying Wei, Wenbing Huang, and Junzhou Huang. Self-supervised graph transformer on large-scale molecular data. *Advances in Neural Information Processing Systems*, 33:12559–12571, 2020.

https://doi.org/10.52202/075280-2540

C. Shannon. The zero error capacity of a noisy channel. *IRE Transactions on Information Theory*, 2(3):8–19, 1956.

Nino Shervashidze, SVN Vishwanathan, Tobias Petri, Kurt Mehlhorn, and Karsten Borgwardt. Efficient graphlet kernels for large graph comparison. In *Artificial intelligence and statistics*, pages 488–495. PMLR, 2009.

Nino Shervashidze, Pascal Schweitzer, Erik Jan Van Leeuwen, Kurt Mehlhorn, and Karsten M Borgwardt. Weisfeiler-lehman graph kernels. *Journal of Machine Learning Research*, 12(9), 2011.

Giannis Siglidis, Giannis Nikolentzos, Stratis Limnios, Christos Giatsidis, Konstantinos Skianis, and Michalis Vazirgiannis. Grakel: A graph kernel library in python. *The Journal of Machine Learning Research*, 21(1):1993–1997, 2020.

Simon Ståhlberg, Blai Bonet, and Hector Geffner. Learning general optimal policies with graph neural networks: Expressive power, transparency, and limits. In *Proceedings of the International Conference on Automated Planning and Scheduling*, volume 32, pages 629–637, 2022.

Fan-Yun Sun, Jordan Hoffmann, Vikas Verma, and Jian Tang. Infograph: Unsupervised and semi-supervised graph-level representation learning via mutual information maximization. *arXiv preprint arXiv:1908.01000*, 2019.

Mingchen Sun, Kaixiong Zhou, Xin He, Ying Wang, and Xin Wang. Gppt: Graph pre-training and prompt tuning to generalize graph neural networks. In *Proceedings of the 28th ACM SIGKDD Conference on Knowledge Discovery and Data Mining*, pages 1717–1727, 2022.

Susheel Suresh, Pan Li, Cong Hao, and Jennifer Neville. Adversarial graph augmentation to improve graph contrastive learning. *Advances in Neural Information Processing Systems*, 34:15920–15933, 2021.

Puja Trivedi, Ekdeep Singh Lubana, Yujun Yan, Yaoqing Yang, and Danai Koutra. Augmentations in graph contrastive learning: Current methodological flaws & towards better practices. In *Proceedings of the ACM Web Conference 2022*, pages 1538–1549, 2022.

Petar Velickovic, William Fedus, William L Hamilton, Pietro Liò, Yoshua Bengio, and R Devon Hjelm. Deep graph infomax. *ICLR (Poster)*, 2(3):4, 2019.

Saurabh Verma and Zhi-Li Zhang. Learning universal graph neural network embeddings with aid of transfer learning. *arXiv preprint arXiv:1909.10086*, 2019.

Chunyu Wei, Jian Liang, Di Liu, and Fei Wang. Contrastive graph structure learning via information bottleneck for recommendation. *Advances in Neural Information Processing Systems*, 35:20407–20420, 2022.

Boris Weisfeiler and Andrei Leman. The reduction of a graph to canonical form and the algebra which appears therein. *NTI, Series*, 2(9):12–16, 1968.

Henry Wolkowicz, Romesh Saigal, and Lieven Vandenberghe. *Handbook of semidefinite programming: theory, algorithms, and applications*, volume 27. Springer Science & Business Media, 2012.

Tailin Wu, Hongyu Ren, Pan Li, and Jure Leskovec. Graph information bottleneck. *Advances in Neural Information Processing Systems*, 33:20437–20448, 2020.

Jiancan Wu, Xiang Wang, Fuli Feng, Xiangnan He, Liang Chen, Jianxun Lian, and Xing Xie. Self-supervised graph learning for recommendation. In *Proceedings of the 44th international ACM SIGIR conference on research and development in information retrieval*, pages 726–735, 2021.

Lingfei Wu, Peng Cui, Jian Pei, Liang Zhao, and Le Song. *Graph neural networks*. Springer, 2022.

Jun Xia, Lirong Wu, Jintao Chen, Bozhen Hu, and Stan Z Li. Simgrace: A simple framework for graph contrastive learning without data augmentation. In *Proceedings of the ACM Web Conference 2022*, pages 1070–1079, 2022.

https://doi.org/10.52202/075280-2540

Teng Xiao, Zhengyu Chen, Zhimeng Guo, Zeyang Zhuang, and Suhang Wang. Decoupled self-supervised learning for graphs. *Advances in Neural Information Processing Systems*, 35:620–634, 2022.

Tian Xie and Jeffrey C Grossman. Crystal graph convolutional neural networks for an accurate and interpretable prediction of material properties. *Physical review letters*, 120(14):145301, 2018.

Junyuan Xie, Ross Girshick, and Ali Farhadi. Unsupervised deep embedding for clustering analysis. In *International conference on machine learning*, pages 478–487. PMLR, 2016.

Yaochen Xie, Zhao Xu, Jingtun Zhang, Zhengyang Wang, and Shuiwang Ji. Self-supervised learning of graph neural networks: A unified review. *IEEE transactions on pattern analysis and machine intelligence*, 2022.

Keyulu Xu, Weihua Hu, Jure Leskovec, and Stefanie Jegelka. How powerful are graph neural networks? *arXiv preprint arXiv:1810.00826*, 2018.

Dongkuan Xu, Wei Cheng, Dongsheng Luo, Haifeng Chen, and Xiang Zhang. Infogcl: Information-aware graph contrastive learning. *Advances in Neural Information Processing Systems*, 34:30414–30425, 2021.

Prateek Yadav, Madhav Nimishakavi, Naganand Yadati, Shikhar Vashishth, Arun Rajkumar, and Partha Talukdar. Lovasz convolutional networks. In *The 22nd international conference on artificial intelligence and statistics*, pages 1978–1987. PMLR, 2019.

Pinar Yanardag and SVN Vishwanathan. Deep graph kernels. In *Proceedings of the 21th ACM SIGKDD international conference on knowledge discovery and data mining*, pages 1365–1374, 2015.

Yihang Yin, Qingzhong Wang, Siyu Huang, Haoyi Xiong, and Xiang Zhang. Autogcl: Automated graph contrastive learning via learnable view generators. In *Proceedings of the AAAI Conference on Artificial Intelligence*, volume 36, pages 8892–8900, 2022.

Yuning You, Tianlong Chen, Yongduo Sui, Ting Chen, Zhangyang Wang, and Yang Shen. Graph contrastive learning with augmentations. *Advances in Neural Information Processing Systems*, 33:5812–5823, 2020.

Yuning You, Tianlong Chen, Yang Shen, and Zhangyang Wang. Graph contrastive learning automated. In *International Conference on Machine Learning*, pages 12121–12132. PMLR, 2021.

Junchi Yu, Tingyang Xu, Yu Rong, Yatao Bian, Junzhou Huang, and Ran He. Recognizing predictive substructures with subgraph information bottleneck. *IEEE Transactions on Pattern Analysis and Machine Intelligence*, 2021.

Jiaqi Zeng and Pengtao Xie. Contrastive self-supervised learning for graph classification. In *Proceedings of the AAAI Conference on Artificial Intelligence*, volume 35, pages 10824–10832, 2021.

Hengrui Zhang, Qitian Wu, Junchi Yan, David Wipf, and Philip S Yu. From canonical correlation analysis to self-supervised graph neural networks. *Advances in Neural Information Processing Systems*, 34:76–89, 2021.

Zaixi Zhang, Qi Liu, Hao Wang, Chengqiang Lu, and Chee-Kong Lee. Motif-based graph self-supervised learning for molecular property prediction. *Advances in Neural Information Processing Systems*, 34:15870–15882, 2021.

Yunhe Zhang, Yan Sun, Jinyu Cai, and Jicong Fan. Deep graph-level orthogonal hypersphere compression for anomaly detection. *arXiv preprint arXiv:2302.06430*, 2023.

Han Zhao, Xu Yang, Zhenru Wang, Erkun Yang, and Cheng Deng. Graph debiased contrastive learning with joint representation clustering. In *IJCAI*, pages 3434–3440, 2021.

https://doi.org/10.52202/075280-2540

A Comaprision with the equivalent forms of the Lovász principles

In this section, we propose an equivalent form of the Lovász principle based on the complement graph of G. We first introduce an equivalent definition of Lovász number as follows.

Definition A.1 (Lovász number Lovász [1979])**.** Let $\bar{G}$ be the complement graph of G and $\bar{\mathcal{U}}$ be the orthonormal representations of $\bar{G}$, Lovász proposed an equivalent definition of Lovász number as

$$\vartheta(G) := \max_{\boldsymbol{d},\boldsymbol{U}\in\bar{\mathcal{U}}} \sum_{p\in V} (\boldsymbol{d}^\top \boldsymbol{u}_p)^2. \tag{19}$$

where $\boldsymbol{d} \in \mathbb{R}^d$ ranges over all unit vectors.

The unit vector $\boldsymbol{d}$ in the Eq. (19) is also a suitable representation vector for graph G. Thus we can obtain a Lovász loss $\bar{\mathcal{L}}_{\text{Lo}}$ based on Definition A.1 as follows.

$$\bar{\mathcal{L}}_{\text{Lo}} := \sum_{i=1}^{|\mathcal{G}|}\left(-\sum_{p\in V_i}\left((\boldsymbol{z}_i^{\phi})^\top \boldsymbol{h}_p^{\theta}\right)^2\right) + \mu\left(\left\|\bar{\boldsymbol{M}}_i \odot \left(\boldsymbol{H}_i^\theta(\boldsymbol{H}_i^\theta)^\top - \boldsymbol{I}_n\right)\right\|_F^2 + \left((\boldsymbol{z}_i^\phi)^\top \boldsymbol{z}_i^\phi - 1\right)^2\right). \tag{20}$$

where $\bar{\boldsymbol{M}}_i = \boldsymbol{A}_i$ is a mask matrix for complement graph $\bar{G}$. Similar to the main paper, an enhanced Lovász loss based on Definition A.1 at iteration t is defined as

$$\bar{\mathcal{L}}_{\text{ELo}}^{(t)} := \bar{\mathcal{L}}_{\text{Lo}}^{(t)} + \lambda\bar{\mathcal{L}}_{\text{SLN}}^{(t)}, \tag{21}$$

where $\bar{\mathcal{L}}_{\text{SLN}}^{(t)}$ is the subgraph Lovász number (SLN) loss of complement graph $\bar{G}$ based on Lovász number definition (19).

We compare the Lovász loss $\bar{\mathcal{L}}_{\text{Lo}}$ and enhanced Lovász loss $\bar{\mathcal{L}}_{\text{ELo}}^{(t)}$ (based on $\boldsymbol{d}$) with the $\mathcal{L}_{\text{Lo}}$ and $\mathcal{L}_{\text{ELo}}^{(t)}$ (based on *handdle* vector $\boldsymbol{c}$). The results are shown in Tables 6, 7 and 8. For convenience, we show the average performance of all methods over all datasets in Figure 3. We see the two equivalent forms of Lovász principles have very similar performance in the three learning tasks and both of them outperform the InfoMax principle.

Table 6: Performance of unsupervised learning. The **bold**, blue and green numbers denote the best, second best, and third best performances respectively, which also applies to Tables 7 and 8.

	methods	MUTAG	PROTEINS	DD	NCI1	COLLAB	IMDB-B	REDDIT-B	REDDIT-M5K
Lovász principle (use $\mathcal{L}_{\text{Lo}}$ and $\boldsymbol{c}$)	InfoGraph	89.67±1.54	75.26±1.43	74.13±1.49	78.21±1.35	71.46±1.21	73.87±1.32	84.76±1.86	54.57±1.38
	GraphCL	87.24±1.96	75.87±2.17	79.14±1.67	79.13±1.27	72.52±1.37	72.44±1.46	89.87±2.13	56.12±1.73
	AD-GCL	87.44±2.13	74.29±2.80	76.25±1.48	75.12±2.13	73.85±1.05	73.02±1.35	87.11±1.95	54.61±2.35
	JOAOv2	87.19±1.92	73.15±1.46	73.15±2.17	74.15±1.67	72.62±1.43	72.18±1.72	84.19±1.67	53.74±1.70
	AutoGCL	89.02±1.47	76.23±1.25	78.95±1.39	82.63±2.12	71.31±1.72	73.95±1.36	89.41±1.81	57.28±1.62
Lovász principle (use $\mathcal{L}_{\text{ELo}}$ and $\boldsymbol{c}$)	InfoGraph	**90.13±2.05**	76.12±1.72	75.76±1.64	79.36±1.57	72.67±1.95	**74.96±1.49**	84.53±1.79	55.12±1.47
	GraphCL	87.93±2.42	**76.82±1.34**	77.35±1.95	80.11±1.47	74.16±1.37	73.87±1.52	90.23±1.87	56.83±1.35
	AD-GCL	88.50±1.82	75.22±1.93	76.14±1.21	78.15±1.81	**74.57±1.98**	73.48±1.41	88.16±1.37	55.64±1.63
	JOAOv2	88.76±1.43	75.27±1.61	74.62±2.58	76.23±1.75	72.85±1.73	72.97±1.37	85.31±1.48	54.68±1.48
	AutoGCL	89.87±1.85	76.03±1.37	79.31±1.27	**82.95±1.26**	72.23±1.52	74.52±1.44	**90.65±1.46**	57.93±1.72
Lovász principle (use $\bar{\mathcal{L}}_{\text{Lo}}$ and $\boldsymbol{d}$)	InfoGraph	88.41±2.47	74.37±2.53	76.26±1.57	77.16±2.43	72.51±1.93	74.12±1.65	86.30±1.92	55.18±2.28
	GraphCL	86.59±1.82	76.42±1.97	78.35±1.42	78.24±1.68	71.46±2.02	73.81±1.92	88.16±1.35	54.75±2.41
	AD-GCL	87.36±1.67	75.10±2.33	76.77±2.10	76.67±1.51	74.24±2.17	73.14±1.51	88.21±2.41	55.42±1.31
	JOAOv2	88.58±2.30	74.26±1.52	75.01±1.65	77.28±1.92	73.21±1.81	73.21±1.95	85.47±2.02	55.09±2.46
	AutoGCL	88.25±2.11	75.78±2.31	77.16±1.91	80.16±1.07	73.11±2.21	74.64±2.07	87.57±2.14	56.83±2.18
Lovász principle (use $\bar{\mathcal{L}}_{\text{ELo}}$ and $\boldsymbol{d}$)	InfoGraph	89.92±1.26	75.37±1.78	76.12±1.81	80.47±1.99	73.18±1.64	73.11±1.38	85.16±2.31	54.87±2.35
	GraphCL	88.93±2.51	75.13±1.26	77.52±2.18	81.35±1.62	73.26±2.01	74.21±1.45	89.47±2.23	55.21±1.92
	AD-GCL	89.38±1.79	76.72±2.09	75.33±1.95	80.02±2.51	74.18±1.44	74.09±1.50	87.36±1.52	56.39±2.32
	JOAOv2	87.30±1.25	74.62±1.30	76.12±1.12	79.14±2.50	73.11±2.30	73.16±1.42	87.69±2.20	55.67±1.83
	AutoGCL	89.31±2.01	75.23±1.46	**79.87±1.34**	82.71±1.34	74.20±1.28	73.90±1.67	90.47±2.52	**58.17±1.68**

B Experimental setting of transfer learning

Following [Hu *et al.*, 2019; You *et al.*, 2021; Yin *et al.*, 2022], we compare the performance of transfer learning of the Lovász principle with the InfoMax principle. We use the Pretrain-GNN method [Hu *et al.*, 2019] as a baseline and employ the Infomax, EdgePred, AttrMasking, and ContextPred pre-training strategies. The experimental settings followed those of AutoGCL [Yin *et al.*, 2022]. Specifically, we performed supervised pre-training for 100 epochs on the ChEMBL dataset [Mayr *et al.*, 2018; Gaulton *et al.*, 2012], and then fine-tuned the model for 30 epochs on 8 chemistry evaluation subsets, using a classifier with a hidden size of 300. Our training employed a batch size of 256 and a learning rate of 0.001. We substitute the InfoMax loss in the four contrastive learning methods (GraphCL, AD-GCL, JOAOv2, and AutoGCL) with the Lovász loss $\mathcal{L}_{\text{Lo}}$ or $\mathcal{L}_{\text{ELo}}$. We repeat each experiment 10 times and report the average ROC-AUC scores in Table 3 of the main paper.

Table 7: Performance of semi-supervised learning.

	methods	NCI1	PROTEINS	DD	COLLAB	REDDIT-B	REDDIT-M5K	GITHUB
Lovász (use $\mathcal{L}_{\text{Lo}}$ and $\boldsymbol{c}$)	GraphCL	75.46±1.53	75.12±1.87	77.46±1.52	76.12±1.15	89.87±1.68	53.69±1.68	66.72±1.53
	AD-GCL	76.62±1.83	74.21±1.71	78.27±1.39	76.27±1.74	90.36±1.56	54.06±1.32	65.32±1.04
	JOAOv2	76.13±1.76	73.73±1.86	76.27±1.48	77.35±1.27	89.31±1.85	53.17±1.76	66.35±1.96
	AutoGCL	75.77±1.48	76.36±1.57	78.16±1.61	77.63±1.78	84.64±2.53	51.31±1.81	64.87±1.62
Lovász (use $\mathcal{L}_{\text{ELo}}$ and $\boldsymbol{c}$)	GraphCL	75.81±1.68	75.88±1.67	78.43±1.48	77.57±1.58	90.67±1.27	54.81±1.73	67.04±1.45
	AD-GCL	77.28±1.04	75.43±1.58	78.67±1.64	76.98±1.87	**91.54±1.39**	55.46±1.59	66.87±1.25
	JOAOv2	76.25±1.59	74.67±1.37	77.96±1.86	78.84±1.75	90.25±1.22	54.32±1.89	**67.52±1.73**
	AutoGCL	76.53±1.92	76.89±1.55	78.82±1.90	78.46±1.39	87.31±1.57	53.17±1.50	66.47±1.26
Lovász (use $\bar{\mathcal{L}}_{\text{Lo}}$ and $\boldsymbol{d}$)	GraphCL	76.21±1.80	76.67±2.14	78.20±1.64	78.26±2.47	90.24±2.13	54.71±1.97	65.91±2.43
	AD-GCL	75.71±1.46	75.39±1.57	77.86±1.77	77.53±1.89	91.14±2.63	54.17±2.75	66.14±1.71
	JOAOv2	76.40±2.32	74.61±1.28	77.26±2.01	76.45±1.34	88.27±1.89	54.34±2.53	65.41±2.76
	AutoGCL	76.84±1.53	76.49±2.03	78.35±1.75	78.02±2.41	86.17±1.61	52.26±1.76	64.26±2.41
Lovász (use $\bar{\mathcal{L}}_{\text{ELo}}$ and $\boldsymbol{d}$)	GraphCL	76.28±1.59	76.21±2.30	**79.34±2.51**	78.10±1.76	91.21±2.04	**55.62±2.68**	66.59±1.62
	AD-GCL	**77.65±2.17**	75.52±1.97	78.71±1.93	77.29±2.33	90.76±2.18	55.14±1.73	67.31±2.41
	JOAOv2	76.19±2.30	75.41±2.24	78.03±2.58	**79.31±1.49**	91.34±2.11	53.70±2.41	66.35±2.28
	AutoGCL	75.42±1.87	**77.25±2.67**	77.54±1.26	78.27±2.43	88.69±2.63	54.28±1.64	66.19±1.67

Table 8: Performance of transfer learning.

	methods	BBBP	Tox21	ToxCast	SIDER	ClinTox	MUV	HIV	BACE
Lovász (use $\mathcal{L}_{\text{Lo}}$ and $\boldsymbol{c}$)	GraphCL	71.37±1.74	75.66±1.82	63.35±1.47	62.11±1.35	77.02±1.67	72.25±1.42	79.23±1.43	78.51±1.58
	AD-GCL	72.24±1.89	77.52±1.74	63.56±1.36	63.87±1.53	80.35±2.36	74.42±1.57	78.95±2.21	80.17±1.04
	JOAOv2	72.16±1.35	75.86±1.21	63.92±1.52	62.56±1.12	81.26±2.37	75.94±1.38	79.01±2.68	79.82±1.39
	AutoGCL	73.79±1.41	76.13±1.48	64.21±1.58	63.24±1.51	81.32±2.12	76.04±1.87	78.64±1.95	82.57±1.95
Lovász (use $\mathcal{L}_{\text{ELo}}$ and $\boldsymbol{c}$)	GraphCL	73.05±1.21	76.45±1.35	64.58±1.73	63.72±1.52	80.21±2.31	74.43±1.95	80.37±1.52	80.63±1.63
	AD-GCL	72.48±1.59	**77.96±1.71**	64.27±1.68	63.91±1.74	81.76±2.01	75.88±1.48	81.08±2.35	82.21±1.49
	JOAOv2	74.13±1.26	76.21±1.35	64.81±1.92	63.38±1.89	**82.75±2.69**	76.51±1.53	81.13±1.96	81.34±1.35
	AutoGCL	74.67±1.81	76.97±1.76	65.36±1.45	64.13±1.48	82.13±2.41	**76.93±1.62**	79.56±1.41	**83.57±1.30**
Lovász (use $\bar{\mathcal{L}}_{\text{Lo}}$ and $\boldsymbol{d}$)	GraphCL	72.53±2.16	75.27±1.35	64.20±1.82	63.16±2.25	79.17±1.63	74.53±2.28	78.61±1.55	80.43±1.77
	AD-GCL	71.45±1.77	76.48±2.03	63.78±2.21	62.85±2.31	79.33±2.49	73.19±1.22	79.42±1.43	78.26±1.47
	JOAOv2	71.78±2.27	75.19±1.87	64.26±1.65	63.27±1.80	81.46±1.83	74.39±2.48	79.59±2.17	80.14±2.51
	AutoGCL	72.52±2.30	76.46±2.33	63.81±2.53	62.84±1.34	80.91±2.27	75.57±2.16	79.35±1.42	81.66±1.60
Lovász (use $\bar{\mathcal{L}}_{\text{ELo}}$ and $\boldsymbol{d}$)	GraphCL	74.54±2.23	76.32±2.54	**65.62±1.74**	**64.34±1.86**	81.75±1.61	75.20±2.31	**81.64±2.37**	81.27±1.58
	AD-GCL	71.74±2.81	77.85±1.95	64.81±2.52	64.25±2.57	80.54±1.32	75.34±1.76	80.56±1.64	81.65±2.48
	JOAOv2	73.71±1.68	76.43±1.64	64.92±2.17	63.56±1.67	81.96±1.58	76.78±1.84	81.53±2.42	80.76±2.31
	AutoGCL	**74.69±2.10**	76.21±1.81	65.13±1.83	63.77±2.52	82.47±2.52	75.42±2.25	80.74±1.56	82.89±2.68

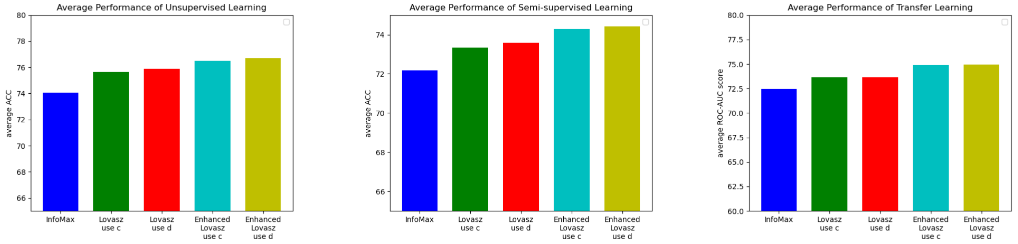

(a) Unsupervised learning (b) Semi-supervised learning (c) Transfer learning

Figure 3: The average performance of different types of methods

C Parameter sensitivity analysis

There are five hyperparameters need to be tuned in Lovász principle method: the dimension of representations d, the hyperparameter of orthonormal representation regularization μ, the hyperparameter of orthogonal regularization in subgraph Lovász number (SLN) loss γ, hyperparameter of subgraph Lovász number (SLN) loss in enhanced Lovász loss η, the hyperparameter of graph-level representations ℓ_2-norm regularization in semi-supervised Lovász loss λ. In this section, we analyze the parameter sensitivity on the InfoGraph Sun *et al.* [2019] with different hyperparameters. We repeat each experiment for ten times and plot the average accuracy on different datasets.

C.1 d as the dimension of representations

In Lovász principle, d is the dimension of node-level representations $\boldsymbol{H} = [\boldsymbol{h}_1, ..., \boldsymbol{h}_n]^\top \in \mathbb{R}^{n\times d}$ and graph-level representation of G, $\boldsymbol{h}_v \in \mathbb{R}^d$. In the definition of Lovász number, the node-level representations are orthonormal representations, i.e., $\boldsymbol{H}^\top \in \mathcal{U}$. Let $\alpha(G)$ be the independent number of graph G, which is the size of the maximum independent set. If $d \leq \alpha(G)$, the node-level representations $\boldsymbol{H}$ are impossible to be orthonormal representations such that the Lovász number cannot be obtained. In Figure 4, we fix other hyperparameters and tune d from $\{10, 20, ..., 90, 100\}$.

https://doi.org/10.52202/075280-2540

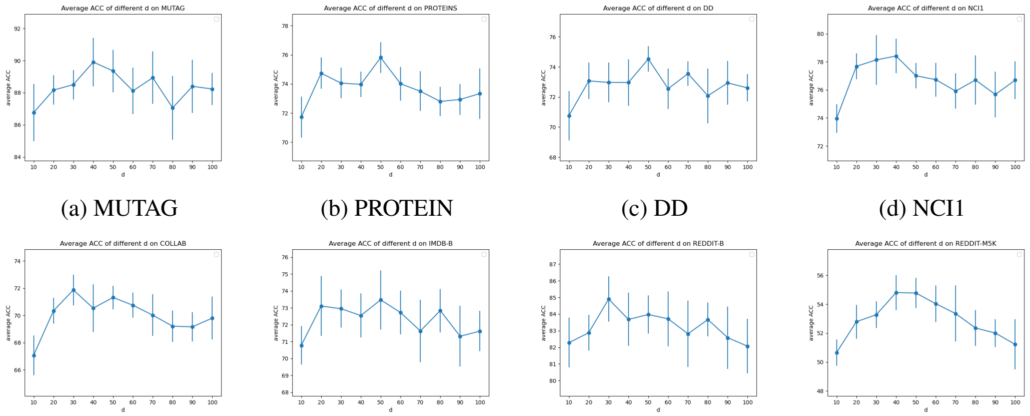

(a) MUTAG (b) PROTEIN (c) DD (d) NCI1

(e) COLLAB (f) IMDB-B (g) REDDIT-B (h) REDDIT-M5

Figure 4: The average ACC of different d on different dataset

The results show that a small d adversely affects the performance because d may be less than $\alpha(G)$ on some graphs. When d is too large, the average accuracy decreases slightly because the representations with large d may capture some noisy information of a graph.

C.2 μ for orthonormal representation regularization

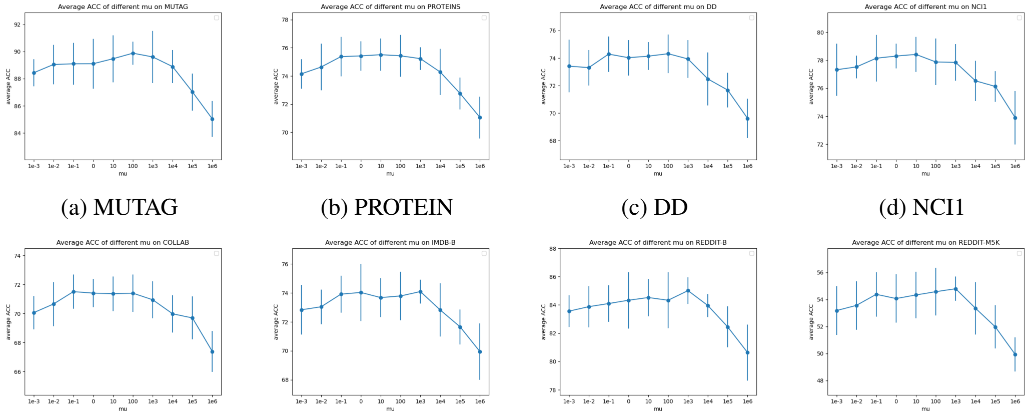

(a) MUTAG (b) PROTEIN (c) DD (d) NCI1

(e) COLLAB (f) IMDB-B (g) REDDIT-B (h) REDDIT-M5

Figure 5: The average ACC of different μ on different data

In Lovász principle, μ is the hyperparameter for orthonormal representation regularization in Lovász loss $\mathcal{L}_{\text{Lo}}$ (9) as follows

$$\mathcal{L}_{\text{Lo}} := \sum_{i=1}^{|\mathcal{G}|} \max_{p \in V_i} \frac{1}{((\boldsymbol{z}_i^{\phi})^\top \boldsymbol{h}_p^{\theta})^2} + \mu \left(\left\| \boldsymbol{M}_i \odot \left(\boldsymbol{H}_i^{\theta} (\boldsymbol{H}_i^{\theta})^\top - \boldsymbol{I}_n \right) \right\|_F^2 + \left((\boldsymbol{z}_i^{\phi})^\top \boldsymbol{z}_i^{\phi} - 1 \right)^2 \right). \quad (22)$$

In Figure 5, we fix other hyperparameters and tune μ from $\{10^{-3}, 10^{-2}, ..., 10^5, 10^6\}$. The results show that μ is not sensitive when $0.1 \leq \mu \leq 1e3$. If μ is too small, the average accuracy decreases slightly because the node-level representations $\boldsymbol{H}$ may not be orthonormal representations. A very large μ adversely affects the performance because the orthonormal representation regularization dominates the representation learning such that the Lovász principle fails.

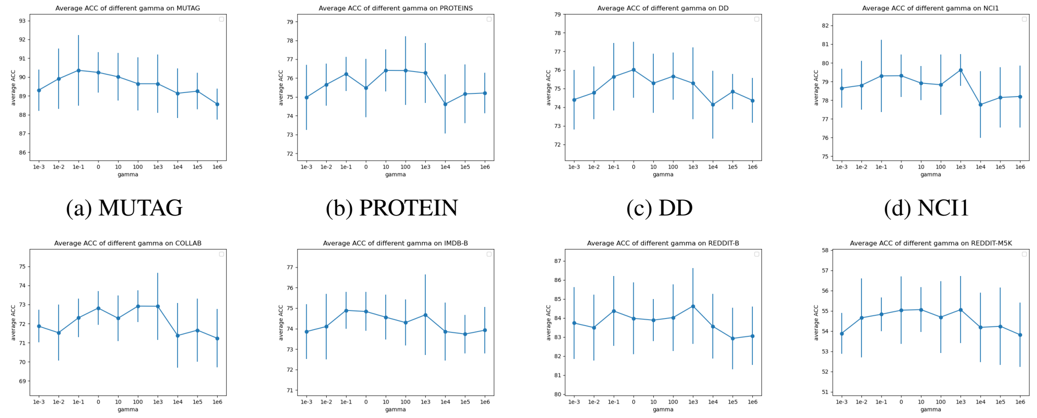

(a) MUTAG (b) PROTEIN (c) DD (d) NCI1

(e) COLLAB (f) IMDB-B (g) REDDIT-B (h) REDDIT-M5

Figure 6: The average ACC of different γ on different data

C.3 γ for orthogonal regularization in subgraph Lovász number (SLN) loss

In Lovász principle, γ is the hyperparameter for orthogonal regularization in subgraph Lovász number (SLN) loss $\mathcal{L}_{\text{SLN}}^{(t)}$ as follows

$$\mathcal{L}_{\text{SLN}}^{(t)} := \sum_{i=1}^{|\mathcal{G}|}\sum_{j=1}^{|\mathcal{G}|} K_{ij}^{(t-1)} \|\boldsymbol{z}_i^{\phi} - \boldsymbol{z}_j^{\phi}\|_2^2 + \gamma(\|\boldsymbol{Z}_{\phi}^{\top}\boldsymbol{Z}_{\phi} - \boldsymbol{I}_d\|_F^2 + \|\boldsymbol{Z}_{\phi}^{\top}\mathbf{1}_{N\times 1}\|_2^2), \tag{23}$$

In Figure 6, we fix other hyperparameters and tune γ from $\{10^{-3}, 10^{-2}, ..., 10^{5}, 10^{6}\}$. The results show that γ is not sensitive when $0.1 \leq \gamma \leq 1e3$. If γ is too small, the average accuracy decreases slightly because the orthogonal constraints of spectral embedding may not hold. A very large γ adversely affects the performance because the orthogonal regularization of spectral embedding dominates the representation learning such that the Lovász principle fails.

C.4 η for subgraph Lovász number (SLN) loss in enhanced Lovász loss

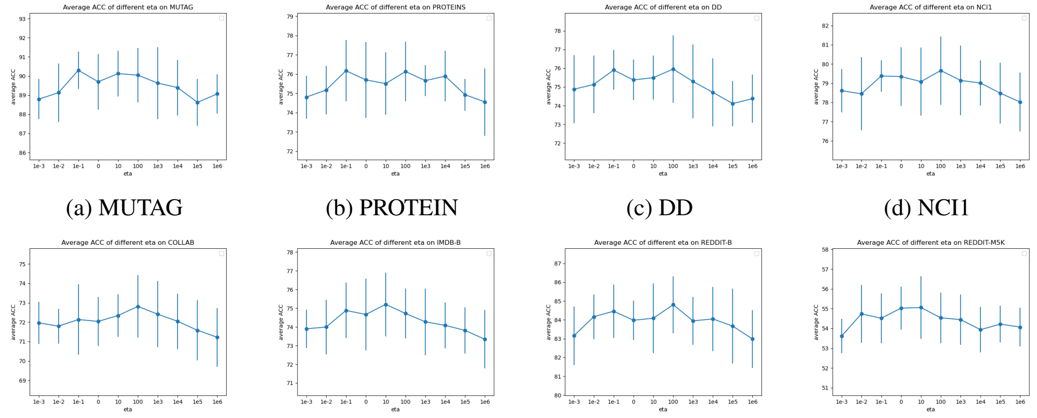

(a) MUTAG (b) PROTEIN (c) DD (d) NCI1

(e) COLLAB (f) IMDB-B (g) REDDIT-B (h) REDDIT-M5

Figure 7: The average ACC of different η on different data

In Lovász principle, η is the hyperparameter for subgraph Lovász number (SLN) loss $\mathcal{L}_{\text{SLN}}^{(t)}$ in enhanced Lovász loss $\mathcal{L}_{\text{ELo}}^{(t)}$ as follows

$$\mathcal{L}_{\text{ELo}}^{(t)} := \mathcal{L}_{\text{Lo}}^{(t)} + \eta\mathcal{L}_{\text{SLN}}^{(t)}.$$

In Figure 7, we fix other hyperparameters and tune η from $\{10^{-3}, 10^{-2}, ..., 10^5, 10^6\}$. The results show that η is not sensitive when $10^{-2} \leq \eta \leq 1e4$. If η is a very small number, the enhanced Lovász loss $\mathcal{L}^{(t)}_{\text{ELo}}$ degenerates into the Lovász loss $\mathcal{L}_{\text{Lo}}$, which also performs well in representation learning. A very large η adversely affects the performance because the subgraph Lovász number (SLN) loss $\mathcal{L}^{(t)}_{\text{SLN}}$ dominates the representation learning such that the Lovász principle may fail.

C.5 λ for the ℓ_2-norm regularization in semi-supervised Lovász loss

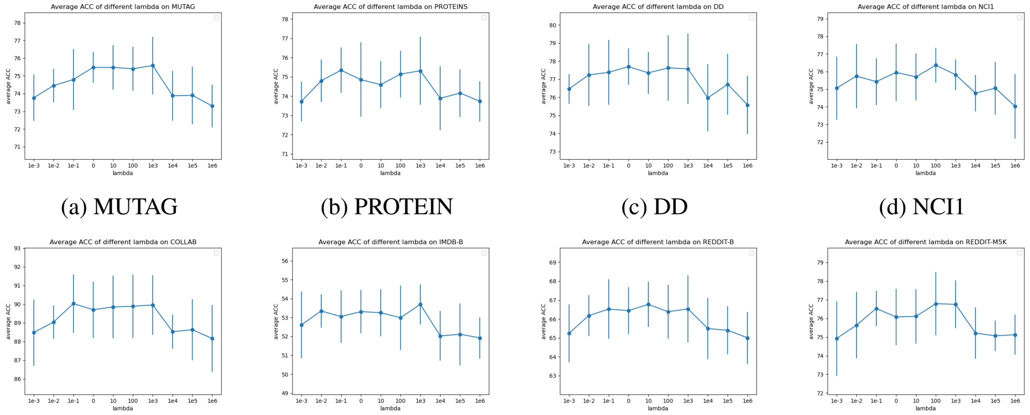

(a) MUTAG (b) PROTEIN (c) DD (d) NCI1

(e) COLLAB (f) IMDB-B (g) REDDIT-B (h) REDDIT-M5

Figure 8: The average ACC of different λ on different data

In semi-supervised learning, λ the hyperparameter for the ℓ_2-norm regularization in semi-supervised Lovász loss as follows

$$\mathcal{L}_{\text{Lo-semi}} := \sum_{l=1}^{|\mathcal{G}^L|} \mathcal{L}_{\text{supervised}}(\hat{\boldsymbol{y}}_l^{\psi}, \boldsymbol{y}_l) + \mathcal{L}_{\text{unsupervised}}(\boldsymbol{H}_i^{\theta}, \boldsymbol{z}_i^{\phi}) + \lambda \sum_{i=1}^{|\mathcal{G}|} \|\boldsymbol{z}_i^{\phi} - \boldsymbol{z}_i^{\psi}\|_2^2, \tag{24}$$

In Figure 8, we fix other hyperparameters and tune λ from $\{10^{-3}, 10^{-2}, ..., 10^5, 10^6\}$. The results show that η is not sensitive when $0.1 \leq \gamma \leq 1e3$. If λ is a very small number, the supervised encoder and unsupervised encoder may learn different information of a graph G such that the average accuracy slightly decreases. A very large η will cause the training to be trapped in early iterations such that the representation learning fails.

D Ablation study

In this section, we analyze the importance of the orthonormal representation regularization (Eq. (9)) and the subgraph Lovász number (SLN) loss (Eq. (14)) by ablation study on unsupervised learning.

D.1 Ablation study of orthonormal representation regularization

In the ablation study, we remove the orthonormal representation regularization in Eq. (9) by setting $\mu = 0$. The results in Table 9 show that the orthonormal representation regularization can improve the performance of graph representation learning for two reasons:

- The orthonormal representation constraint is part of the definition of Lovász number such that the Lovász principle may fail without the orthonormal representation regularization.
- The orthonormal representation regularization guides the method the learn the structure property of a graph.

Table 9: Performance (ACC) of unsupervised learning for Ablation study. The ablation indicates $\mu = 0$ in Eq. (9). The **bold** numbers denote the better performances of the same method.

	methods	ablation	MUTAG	PROTEINS	DD	NCI1	COLLAB	IMDB-B	REDDIT-B	REDDIT-M5K
Lovász principle (use $\mathcal{L}_{\text{Lo}}$)	InfoGraph	✓	88.25±1.63	74.38±1.52	73.05±1.77	76.89±1.42	**72.23±1.35**	72.09±1.41	83.56±1.22	53.21±1.90
		×	**89.67±1.54**	**75.26±1.43**	**74.13±1.49**	**78.21±1.35**	71.46±1.21	**73.87±1.32**	**84.76±1.86**	**54.57±1.38**
	GraphCL	✓	86.16±1.31	73.48±1.56	78.22±1.09	77.84±1.73	71.65±1.20	71.82±1.78	87.79±1.86	55.03±2.17
		×	**87.24±1.96**	**75.87±2.17**	**79.14±1.67**	**79.13±1.27**	**72.52±1.37**	**72.44±1.46**	**89.87±2.13**	**56.12±1.73**
	AD-GCL	✓	86.28±1.84	73.52±1.78	75.89±1.67	74.53±1.36	72.41±1.58	72.84±1.52	**88.46±1.35**	53.27±1.51
		×	**87.44±2.13**	**74.29±2.80**	**76.25±1.48**	**75.12±2.13**	**73.85±1.05**	**73.02±1.35**	87.11±1.95	**54.61±2.35**
	JOAOv2	✓	**88.34±1.36**	72.49±1.19	72.53±2.07	73.64±2.52	72.27±1.59	71.63±1.81	83.48±1.31	53.02±1.21
		×	87.19±1.92	**73.15±1.46**	**73.15±2.17**	**74.15±1.67**	**72.62±1.43**	**72.18±1.72**	**84.19±1.67**	**53.74±1.70**
	AutoGCL	✓	88.76±2.15	75.59±2.03	78.42±1.81	81.79±1.65	70.42±1.30	73.64±1.52	88.31±1.22	56.53±1.27
		×	**89.02±1.47**	**76.23±1.25**	**78.95±1.39**	**82.63±2.12**	**71.31±1.72**	**73.95±1.36**	**89.41±1.81**	**57.28±1.62**
Lovász principle (use $\mathcal{L}_{\text{ELo}}$)	InfoGraph	✓	89.51±1.63	75.18±1.67	**76.29±1.52**	78.24±1.61	71.22±1.43	74.35±1.07	83.87±2.39	**56.23±1.15**
		×	**90.13±2.05**	**76.12±1.72**	75.76±1.64	**79.36±1.57**	**72.67±1.95**	**74.96±1.49**	**84.53±1.79**	55.12±1.47
	GraphCL	✓	86.78±1.57	76.24±1.60	76.71±1.63	79.42±1.03	73.37±1.26	73.42±1.07	89.70±1.52	55.64±1.25
		×	**87.93±2.42**	**76.82±1.34**	**77.35±1.95**	**80.11±1.47**	**74.16±1.37**	**73.87±1.52**	**90.23±1.87**	**56.83±1.35**
	AD-GCL	✓	88.36±1.51	74.63±1.74	**76.39±1.37**	77.68±1.23	74.03±1.52	72.73±1.22	87.31±1.21	**55.87±1.42**
		×	**88.50±1.82**	**75.22±1.93**	76.14±1.21	**78.15±1.81**	**74.57±1.98**	**73.48±1.41**	**88.16±1.37**	55.64±1.63
	JOAOv2	✓	88.27±1.39	74.52±1.40	74.31±1.15	75.78±1.43	72.10±1.62	72.39±2.15	84.45±1.36	**54.21±1.52**
		×	**88.76±1.43**	**75.27±1.61**	**74.62±2.58**	**76.23±1.75**	**72.85±1.73**	**72.97±1.37**	**85.31±1.48**	54.68±1.48
	AutoGCL	✓	89.24±2.43	75.29±1.58	78.42±1.68	82.31±1.79	71.69±1.98	**74.46±1.65**	90.10±1.73	57.27±1.54
		×	**89.87±1.85**	**76.03±1.37**	**79.31±1.27**	**82.95±1.26**	**72.23±1.52**	74.52±1.44	**90.65±1.46**	**57.93±1.72**

D.2 Ablation study of subgraph Lovász number (SLN) loss

If we remove the subgraph Lovász number (SLN) loss in Eq. (14) by setting $\eta = 0$, the enhanced Lovász loss (14) degenerates to simple Lovász loss (9). The results in Table 10 show that the subgraph Lovász number (SLN) loss can improve the performance of graph representation learning because similar graphs are guaranteed to be close to each other in the representation space.

D.3 Ablation study of orthonormal representation regularization

Table 10: Performance (ACC) of unsupervised learning for Ablation study. The ablation indicates $\eta = 0$ in Eq. (14). The **bold** numbers denote the better performances of the same method.

methods	ablation	MUTAG	PROTEINS	DD	NCI1	COLLAB	IMDB-B	REDDIT-B	REDDIT-M5K
InfoGraph	✓	89.67±1.54	75.26±1.43	74.13±1.49	78.21±1.35	71.46±1.21	73.87±1.32	**84.76±1.86**	54.57±1.38
	×	**90.13±2.05**	**76.12±1.72**	**75.76±1.64**	**79.36±1.57**	**72.67±1.95**	**74.96±1.49**	84.53±1.79	**55.12±1.47**
GraphCL	✓	87.24±1.96	75.87±2.17	**79.14±1.67**	79.13±1.27	72.52±1.37	72.44±1.46	89.87±2.13	56.12±1.73
	×	**87.93±2.42**	**76.82±1.34**	77.35±1.95	**80.11±1.47**	**74.16±1.37**	**73.87±1.52**	**90.23±1.87**	**56.83±1.35**
AD-GCL	✓	87.44±2.13	74.29±2.80	**76.25±1.48**	75.12±2.13	73.85±1.05	73.02±1.35	87.11±1.95	54.61±2.35
	×	**88.50±1.82**	**75.22±1.93**	76.14±1.21	**78.15±1.81**	**74.57±1.98**	**73.48±1.41**	**88.16±1.37**	**55.64±1.63**
JOAOv2	✓	87.19±1.92	73.15±1.46	73.15±2.17	74.15±1.67	72.62±1.43	72.18±1.72	84.19±1.67	53.74±1.70
	×	**88.76±1.43**	**75.27±1.61**	**74.62±2.58**	**76.23±1.75**	**72.85±1.73**	**72.97±1.37**	**85.31±1.48**	**54.68±1.48**
AutoGCL	✓	89.02±1.47	**76.23±1.25**	78.95±1.39	82.63±2.12	71.31±1.72	73.95±1.36	89.41±1.81	57.28±1.62
	×	**89.87±1.85**	76.03±1.37	**79.31±1.27**	**82.95±1.26**	**72.23±1.52**	**74.52±1.44**	**90.65±1.46**	**57.93±1.72**

E Strict Lovász Principle

We use regularization in Lovász principle (9) instead of constraint because its optimization is much easier and its performance is very close to the constrained optimization. In Algorithm 1, we propose a constrained optimization for the "strict Lovász principle" via projection.

Algorithm 1: Constrained optimization for "strict Lovász principle"

```
Initialization: $\mu = 1$
repeat
    $\hat{H}^t = F(A, X; \theta^t)$ and $\hat{z}^t = f(A, X; \phi^t)$
    $H^t = \text{Proj}_U(\hat{H}^t)$ and $z^t = \frac{\hat{z}^t}{\|\hat{z}^t\|}$
    obtain $\theta^{t+1}, \phi^{t+1}$ by SGD updating
until Convergence
```

In Algorithm 1, the Proj_U project $\hat{H}^t$ to the orthonormal representation space, which is similar to the Gram–Schmidt process. We define $\text{proj}_w(h) := \frac{<h,w>}{<w,w>}w$. Let W_k be the set that $W_k := \{w_1, w_2, ..., w_k\}$. For each vertex $i \in V$, we denote Ω_i as the set of vector w_js where j can be each vertex not adjacent to vertex i. Then the $H^t = \text{Proj}_U(\hat{H}^t)$ is defined in Algorithm 2

Algorithm 2: The definition of projection function Proj_U

```
$w_1 = \hat{h}_1^t,\ e_1 = \frac{w_1}{\|w_1\|}$
$w_2 = \hat{h}_2^t - \sum_{w \in W_{2-1} \cap \Omega_2} \mathrm{proj}_w(\hat{h}_2^t),\ e_2 = \frac{w_2}{\|w_2\|}$
...
$w_k = \hat{h}_k^t - \sum_{w \in W_{k-1} \cap \Omega_k} \mathrm{proj}_w(\hat{h}_k^t),\ e_k = \frac{w_k}{\|w_k\|}$
...
$w_n = \hat{h}_n^t - \sum_{w \in W_{n-1} \cap \Omega_n} \mathrm{proj}_w(\hat{h}_n^t),\ e_n = \frac{w_n}{\|w_n\|}$
Output $H^{t+1} = [e_1, e_2, ..., e_n]^\top$
```

The comparisons between the regularized ($\mu = 1$) optimization and the constrained optimization for two methods on four datasets are as follows.

Table 11: Comparison between regularized optimization and constrained optimization

	method	MUTAG	PROTEINS	DD	NCI1
regularized opt.	InfoGraph	89.67± 1.54	75.26 ± 1.43	74.13± 1.49	78.21± 1.35
regularized opt.	GraphCL	87.24±1.96	75.87± 2.17	79.14 ± 1.67	79.13± 1.27
constrained opt.	InfoGraph	86.12± 2.32	75.49± 1.52	76.42± 1.56	77.80± 1.24
constrained opt.	GraphCL	87.52 ± 2.75	76.11± 1.36	78.54 ± 2.21	77.63± 1.58

F Time cost comparison

We compare the time cost between the InfoMax principle and Lovász principle using the InfoGraph Sun *et al.* [2019] model on different datasets. We run the programming on a machine with Intel 7 CPU and RTX 3090 GPU. We repeat the experiment five times and report the results in Table 12. The Lovász principle is the fastest method among the three. The Lovász principle is the fastest method among the three, and the reasons are as follows:

Table 12: Time cost of InfoGraph. h stands for hour and m stands for minute. The brown value indicates the lowest time cost.

tasks	principle	MUTAG	PROTEINS	DD	NCI1	COLLAB	IMDB-B	REDDIT-B	REDDIT-M5K
unsupervised learning	InfoMax	2.3 m	12.6 m	1 h 39 m	36.5 m	1 h 50 m	5.8 m	3 h 14 m	7 h 31 m
	Lovász	1.8 m	11.7 m	1 h 25 m	33.2 m	1 h 46 m	5.1 m	3 h 9 m	7 h 26 m
	Enhanced Lovász	1.8 m	12.2 m	1 h 30 m	34.3 m	1 h 47 m	5.3 m	3 h 10 m	7 h 27 m
semi-supervised learning	InfoMax	2.3 m	13.1 m	1 h 47 m	46.3 m	2 h 21 m	9.6 m	3 h 47 m	8 h 52 m
	Lovász	2.0 m	12.7 m	1 h 39 m	43.1 m	2 h 15 m	8.1 m	3 h 27 m	8 h 16 m
	Enhanced Lovász	2.0 m	12.8 m	1 h 40 m	42.6 m	2 h 17 m	8.3 m	3 h 29 m	8 h 20 m

- The Lovász principle is faster than the InfoMax principle because the former does not use the f-GAN [Nowozin *et al.*, 2016] and the Jensen-Shannon MI estimator I_φ to evaluate the mutual information.
- Enhanced Lovász principle is slightly lower than Lovász principle because the computation of $1/(\boldsymbol{z}_i^{(t-1)\top}\boldsymbol{u}_p^{(t-1)})^2$ for every $p \in V_i$ was already done when computing $\mathcal{L}_{\mathrm{Lo}}$.